Unravelling the Mechanism of TrkA-Induced Cell Death by Macropinocytosis in Medulloblastoma Daoy Cells

Chunhui Li[*], James I.S. MacDonald[*], Asghar Talebian[†], Jennifer Leuenberger[†], Claudia Seah[*], Stephen H. Pasternak[*§], Stephen W. Michnick[¶] and Susan O. Meakin [†, ‡, +]

[*]**Robarts Research Institute and** [§]**Dept. of Clinical Neurological Sciences, Schulich School of Medicine,** [†]**Dept. of Biochemistry and** [‡]**Grad. Prog. in Neurosci., Western University, London, ON, Canada, N6A 5C1.** [¶]**Départ. de Biochimie, Université de Montreal, Montreal, Quebéc, Canada H3T 1J4**

[+] **Corresponding Author.**

Correspondence Footnote: smeakin@uwo.ca

Abbreviations: CA (constitutively active), CK1 (Casein kinase 1), DN (dominant negative), FRS2 (fibroblast growth factor receptor substrate 2), GGA3 (Golgi-localized gamma ear-containing Arf-binding protein), Gb (Glioblastoma), Med (medulloblastoma), NB (Neuroblastoma), NGF (nerve growth factor), PH (pleckstrin homology), PIP_2 (phosphatidylinositol [4,5]-bisphosphate), PIP_3 (phosphatidylinositol [3,4,5]-triphosphate), PIP_5K (phosphatidylinositol 4-phosphate 5-kinase), PI3 kinase (phosphatidylinositol 3 [PI3] kinase), PLC (phospholipase C), PKC (protein kinase C).

Footnote: J. Leuenberger[ǂ], A. Talebian[ƚ]. [ǂ]Canadawide Scientific, 2300 Walkley Road, Ottawa, Ont. [ƚ]Univ. Texas Southwestern Medical Center, 5323 Harry Hines Blvd, Dallas, Texas.

Running Title: H-Ras Drives Cell Death in Medulloblastoma Tumors

Character Count: Abstract, Intro, Results, Discussion and Figure Legends (39,515)

Abstract

Macropinocytosis is a normal cellular process by which cells internalize extracellular fluids and nutrients from their environment and is one strategy that Ras-transformed pancreatic cancer cells use to increase uptake of amino acids to meet the needs of rapid growth. Paradoxically, in non-Ras transformed medulloblastoma brain tumors, we have shown that expression and activation of the receptor tyrosine kinase TrkA over-activates macropinocytosis resulting in the catastrophic disintegration of the cell membrane resulting in tumor cell death. The molecular basis of this uncontrolled form of macropinocytosis has not been previously understood. Here, we demonstrate that the over-activation of macropinocytosis is caused by the simultaneous activation of two TrkA-mediated pathways: (1) inhibition of RhoB *via* phosphorylation at Ser^{185} by casein kinase 1, which relieves actin stress fibers, and (2) FRS2-scaffolded Src and H-Ras activation of RhoA which stimulates actin re-organization and the formation of lamellopodia. Since catastrophic macropinocytosis results in brain tumor cell death, improved understanding of the mechanisms involved will facilitate future efforts to re-program tumors, even those resistant apoptosis, to die.

Introduction

Medulloblastomas (Med) and neuroblastomas (NB) represent two of the most common childhood neoplasias of the central and peripheral nervous systems (1);(2). Med's arise from progenitor cells in the cerebellum (3) while NB's arise from undifferentiated sympathoadrenal cells of neural crest origin (2);(4). In general, the age of onset for both Med and NB is an important determinate of final prognosis with complete regression often being reported in children under one year of age. In contrast, tumors that arise in older children often become metastatic and highly resistant to conventional therapies (5). Two markers, the expression of which correlate with positive prognosis in both Med and NB, are the closely related receptor tyrosine kinases TrkA and TrkC (6);(5);(7). In contrast, expression of TrkB correlates with enhanced drug resistance, MYCN expression, angiogenesis (5) and is a poor prognostic predictor of NBs and it also facilitates cell survival and proliferation in Med's (8).

The relationship between Trk receptor expression and the final prognostic outcome has been linked to the induction of cell death. In many instances, in both primary as well as established Med, NB and glioblastoma (Gb) cell lines, expression of either TrkA or TrkC has been linked to the induction of either apoptosis or autophagy (1);(9);(10);(11);(12). In contrast, we have shown that nerve growth factor (NGF) treatment of Med Daoy cells that over-express TrkA (Daoy-TrkA) show a dramatic increase in uncontrolled macropinocytosis, causing catastrophic disintegration of cellular membrane integrity, resulting in cell death (13). No evidence of apoptosis or necrosis is observed, and although evidence of autophagy is present, siRNA mediated knockdown of the key autophagy proteins, beclin and atg5, does not prevent cell death (13).

69 Macropinocytosis is an actin-dependent, clathrin-independent, endocytic process that can be
70 triggered by external stimuli and serves as a means for cells to take up large amounts of
71 extracellular materials as nutrients (14);(15);(16). Under normal conditions, macropinocytosis
72 can also facilitate receptor mediated signaling pathways, the entry of viral and bacterial
73 pathogens, cell motility (16) and is the mechanism by which macrophages and dendritic cells
74 internalize antigens and cellular debris (17);(16). More recently, macropinocytosis has also been
75 shown to facilitate the uptake of amino acids in Ras-transformed pancreatic tumor cells to sustain
76 their uncontrolled proliferation (14). Macropinosomes are generated by the formation of cell
77 surface lamellipodia that fold back on themselves resulting in large endosomes, which can be
78 larger than 0.2 μm in diameter (18). Under normal physiological conditions, macropinosomes
79 are either recycled back to the cell surface or they fuse with lysosomes to digest internalized
80 nutrients (15);(16). By comparison, the macropinosomes generated in NGF treated Daoy-TrkA
81 cells internally fuse, growing uncontrollably larger and in turn fuse with lysosomes (13). The
82 cells literally drink and eat themselves to death.
83 In addition to our observations in Meds, hyperstimulation of macropinocytosis has also been
84 found to result in cell death in some human Gb cell lines as well as in other cancer cell lines
85 (19);(20);(21);(22). Interestingly, over-expression of oncogenic H-Ras has been shown to drive
86 cell death by macropinocytosis in the Gb cell line, U251 (20);(13), by a mechanism that is
87 dependent upon activation of the GTPase Rac1 and the inactivation of Arf6 (23).
88 Herein, we characterize the signaling mechanisms that drive TrkA-dependent cell death by
89 macropinocytosis in Daoy cells. We find that, similar to U251 cells, induction of
90 macropinocytosis-dependent cell death requires the activation of H-Ras; however, unlike U251
91 cells, it does not depend on the activation of Rac1 or Cdc42.

Moreover, we find that over-expression of constitutively active (CA) H-Ras, alone, is sufficient to activate macropinocytosis-dependent cell death. While it may seem surprising that CA-H-Ras can stimulate cell death in a brain tumor cell line, it is important to note that activating mutations of either H-Ras, N-Ras or K-Ras *have not* been found in cancers of the brain (24)[,](25). In terms of understanding the mechanisms driving this process, we demonstrate the concomitant requirement of several signaling pathways. First, we find that activation of Src is essential, which is known to precede activation of H-Ras (26), and that this is mediated *via* the adapter protein FRS2, not ShcA, which competitively bind to the juxtamembrane phosphorylated tyrosine residue, $pTyr^{490/499}$ on activated TrkA (27). Second, we show that two Rho family GTPases, RhoA and RhoB, are the endpoint effectors and they serve essential, but opposite roles in regulating macropinocytosis. Finally, we have identified an essential role for the serine/threonine kinase casein kinase 1 (CK1) in a mechanism that involves the phosphorylation of RhoB at Ser^{185}. This single event inactivates RhoB (28), releasing actin stress fibres, and enables RhoA to re-organize actin into the lamellopodial extensions required to generate macropinosomes.

Materials and Methods

Antibodies and Growth Factors. The antibodies to β-actin and Arf6 were from Sigma-Aldrich. Antibodies to Cdc42, FRS2, H-Ras, N-Ras, Rap1, RhoB and Sck (ShcB) were from Santa Cruz Biotechnology. Antibodies to RhoA, phospho-Src (Tyr^{416}), phosphor-Src (Tyr^{547}) and anti-phosphoTrkA (Tyr^{490}) antibodies were from Cell Signaling Technology. Antibodies to ShcA, ShcC and Rac1 were from BD Bioscience. The antibody to K-Ras was from Abcam and the antibody to v-src was from Calbiochem. Horseradish peroxidase (HRP) coupled secondary antibodies (rabbit anti-mouse; goat anti-rabbit) were from Jackson ImmunoResearch Labs, Inc.

and used at a final concentration of 1:10,000. Antibodies were used at working concentrations as indicated: anti-β-actin (1:10,000), anti-phosphoTrkA (Tyr^{490}) (1:2000), phospho-Src (Tyr^{416}) (1:5000), phosphor-Src (Tyr^{547}) (1:2000), anti-ShcA (1:5000), anti-ShcC (1:10,000), anti-ShcB (1:1000), anti-FRS2 (1:2000), anti-v-src (1:1000), anti-GST-HRP (1:5000), anti-Ras (1:1000), anti-Rac (1:1000), anti-Cdc42 (1:5000), anti-Arf6 (1:1000), anti-RhoA (1:1000), anti-RhoB (1:500) and anti-Rap1 (1:1000). Nerve growth factor (NGF) was from Harlan Products for Bioscience.

Vectors and Cloning. CA-Rac1 ($Q^{61}L$) was generated by site directed mutagenesis using Pfu Turbo (Stratagene). Human H-Ras cDNA was obtained by PCR amplification from human placenta cDNA and subcloned into pEGFP-C1. CA-H-Ras ($G^{12}V$)-EGFP was generated using human CA-H-Ras as a template by site directed mutagenesis using Pfu Turbo. All other constructs were provided by the following investigators: EGFP-tagged DN ($T^{19}L$) and CA ($Q^{63}L$) RhoB (Dr. A. Richmond, Vanderbilt University School of Med, TN, USA); EGFP-tagged DN ($T^{66}N$) and CA ($Q^{111}L$) Rab34 (Dr. T. Endo, Chiba University, Chiba, Japan); EGFP-tagged CA ($G^{12}V$) and DN ($T^{17}N$) Cdc42, DN ($S^{17}N$) Rac, DN ($K^{44}A$) Dynamin 2, DN ($T^{31}N$) Arf1, YFP-tagged DN ($N^{19}L$) RhoA, DN ($S^{34}N$) Rab5, DN ($T^{22}N$) Rab7 and EGFP- tagged Clathrin (Dr. S. Ferguson, Univ. Ottawa, On, CA); EGFP-tagged DN ($S^{17}N$) and CA ($G^{12}V$) Rap1b (Dr. P. Stork, Vollum Institute, OR, USA); pYFP tagged DN ($S^{147}A$) CtBP1/BARS (Alberto Luini, Inst. of Protein Biochemistry, NRC, Naples, Italy); EGFP tagged DN ($T^{17}N$) and CA ($Q^{61}L$) Arf6 (Dr. J. Donaldson, NIH, MD, USA); constructs encoding the pleckstrin homology (PH) domains of PLCδ and Akt fused with EGFP and the Ras binding domain (RBD) cysteine-rich domain (CRD) domain of c-Raf-1fused with EGFP (Dr. T. Balla, NIH, MD, USA); EGFP-tagged cRaf-1 CRD ($R^{89}A$) mutant (Dr. Y. Sako, RIKEN ASI, Japan); EGFP tagged DN-Src516

(1-516) (Dr. N. Yamaguchi, Chiba Univ., Japan); EGFP-RhoB ($S^{185}A$) (Dr. A. Pradines, INSERM, Toulouse, France) and the GFP-RhoA binding domain of Rhoteckin to visualize active RhoA (GFP-rGBD) (Dr. W. Bement, Addgene ID-26740 and 26732). pGex vectors expressing GST fusions encoding binding domains for specific GTPases were obtained from the following investigators: RBD of c-Raf (Raf-RBD) (Dr. D. Shalloway, UC Berkeley, CA, USA); Cdc42/Rac-interacting binding (CRIB) domain of p21-activated kinase-1 (Pak1) (Dr. A. Hall, Memorial Sloan-Kettering Cancer Center, NY, USA); RBD of RalA (RalGDS-RBD, Dr. P. Stork, Vollum Institute, OR, USA); Rho binding domain of RHOteckin-RBD (Dr. A. Richmond, Vanderbilt Univ., TN, USA); N-terminal GAT domain of the Golgi-localized gamma ear-containing Arf-binding protein 3 (GGA3) which binds activated Arf6 (Dr. M. Park, McGill Univ., Montreal, CA).

Cell Culture and Transfections. Daoy-TrkA cells were provided by Dr. V. Lee (Univ. of Pennsylvania, USA) and maintained in Dulbecco's minimal eagle medium (DMEM) supplemented with 10% fetal bovine serum, 100 µg/ml gentamycin sulfate and 100 µg/ml G418. Daoy cells were grown in the same media without G418. Cells were routinely transfected with 4-10 µg of plasmid or 20 nM siRNA's using Lipofectamine 2000 (Life Technologies) or DreamFect Gold (OZ Biosciences) following specifications of the manufacturer.

Small Interfering RNAs. Validated or sequence specific siRNAs were generated and purchased from Life Technologies against the following targets: (i) human H-Ras (validated stealth siRNA VHS40291), (ii) human FRS2 (sense CUG GCU AUG ACA GUG AUG AAC GAA G; antisense CUU CGU UCA UCA CUG UCA UAG CCA G), (iii) Src (sense AAC AAG AGC AAG CCC AAG GAU; antisense AUC CUU GGG CUU GCU CUU GUU) (29), (iv) human ShcA (silencer select 4390827; sense CUA CUU GGU UCG GUA CAU Ggg; antisense CAU

GUA CCG AAC CAA GUA Gga), (v) human Rac1 (sense UUU GAC AGC ACC GAU CUC UUU CGC C; antisense GGC GAA AGA GAU CGG UGC UGU CAA A), (vi) human Cdc42 (sense UCC UUU CUU GCU UGU UGG GAC UCA A; antisense UUG AGU CCC AAC AAG CAA GAA AGG A) (30), (vii) human RhoB (sense CCG UCU UCG AGA ACU AUC UUU; antisense AGA UAG UUC UCG AAG ACG GUU), (viii) a stealth control (sense GAG UCG ACC UAG UGU AAC ACC GAC A; antisense UGU CGG UGU UAC ACU AGG UCG ACU C). Cy3-labelled negative control siRNA (Life Technologies) was co-transfected with test siRNAs to monitor transfection efficiency.

Inhibitor/Dyes. Daoy-TrkA cells were pre-treated with the following inhibitors 1 hour prior to NGF stimulation (100 ng/ml) unless otherwise stated: 40 µM of the CK1 inhibitor, D4476 (Calbiochem), 5-10 µM of the Rac1 inhibitor EHT1864 (Tocris Bioscience), 2 µg/ml of the Rho inhibitor CT04 (Cytoskeleton, Inc). The Src inhibitor PP2 (Sigma-Aldrich) was used at the concentrations indicated. Dimethyl sulfoxide (DMSO) was used as a negative control. Alexa Fluor^{546}-Dextran, Alex Fluor^{488}-Dextran and Alexa Fluor^{546}-transferrin (Life Technologies) were used at a final concentration of 5 µg/ml (dextran) or 50 µg/ml (transferrin).

GTPase binding Assays. pGex2T, pGex2T-PAK-CRIB, pGex-Raf1-RBD, pGex-RalGDS-RBD, pGex-RHOteckin-RBD and pGex-GGA3-NGAT were grown in 50 ml Luria broth (LB) with 50 µg/ml ampicillin for 16 h at 37° C then added to 500 ml of LB with 50 µg/ml ampicillin and grown to an OD_{600} of 0.8 to 1.0. Cultures were induced with IPTG (0.2 mg/ml) for 2 h at 37° C, centrifuged at 5000 rpm for 10 min (4° C), re-suspended in 10 ml 1X PBS and frozen at -80°C. Pellets were re-suspended in 20 ml of re-suspension buffer (25 mM Tris-Cl pH 7.5, 5 mM EDTA pH 8.0, 150 mM NaCl, 1 mM PMSF, 1 µg/ml leupeptin). Cells expressing the PAK-Crib domain were lysed by two passages through a pre-chilled French press at 20,000 psi. Triton X-

100 was added to a final concentration of 1% and the sample rotated for 30 min at 4°C. All other GST fusions were re-suspended as described above and lysed directly by the addition of Triton X-100 to a final concentration of 1%. Samples were centrifuged at 14,000 rpm for 10 min at 4 °C. Washed glutathione agarose (500 µl) (Sigma-Aldrich) was added to the supernatant and the mixtures incubated for 16 h at 4°C followed by three washes with 10 ml 1X PBS and re-suspended in 250 µl interaction buffer (20 mM Hepes, 150 mM NaCl, 0.05% NP40, 10% glycerol, 1 mM PMSF, 1 µg/ml leupeptin). To measure changes in GTP activation, Daoy-TrkA cells were left untreated or stimulated with NGF (100 ng/ml) for 10 min, 6 h, 12 h and 24 h. Prior to lysis, cells were placed on ice, washed with ice-cold phosphate buffered saline (PBS), lysed in 500 µl interaction buffer (containing 100 µM GTPγS, 10 µg/ml aprotinin, 2 µg/ml leupeptin and 1 mM PMSF) for 2 min and lysates centrifuged at 10,000 rpm for 10 min at 4°C. Protein concentrations of lysates were determined with the DC Protein Assay Kit (BioRad) and the main lysates flash frozen in liquid nitrogen and stored at -80^{o}C until use. Purified GST fusion proteins (approximately 30 µg) were added to 500-1000 µg of un-stimulated and NGF-stimulated Daoy-TrkA lysates and incubated at 4 °C for 16 h (1 h for RhoA). Samples were pelleted at 14,000 rpm at 4^{o}C and washed twice with interaction buffer. Laemmli sample buffer with 100 mM DTT was added and samples heated at 70°C for 10 min. Proteins were analyzed by 12% SDS-PAGE and blotted with anti-GST-HRP (1:5000), anti-H-Ras (1:1000), anti-Rac1 (1:1000), anti-Cdc42 (1:5000), anti-Arf6 (1:1000), anti-RhoB (1:500), anti-RhoA (1:1000) and anti-Rap1 (1:1000) antibodies. Lysates from each time point (25 µl) were also assayed for changes in the expression of each GTPase relative to β-actin as a control.

Immunoprecipitation and Western Blotting. Daoy-TrkA cells were stimulated with NGF (100 ng/ml), washed twice with ice cold PBS containing 1mM sodium orthovanadate and lysed

in NP-40 lysis buffer (1% NP-40, 137 mM NaCl, 10% glycerol, 1 mM EDTA, 50 mM Tris-HCl, pH 8.0) containing 1 mM sodium orthovanadate, 10 mM NaF, 10 µg/ml aprotinin, 2 µg/ml leupeptin and 1 mM PMSF. Clarified supernatants were collected by centrifugation and lysates (500 µg) were immunoprecipitated with an antibody to TrkA and Gamma-bind Plus Sepharose (Amersham Pharmacia Biotech). Immune complexes were collected by centrifugation after an overnight incubation at 4°C, washed and re-suspended in SDS-PAGE sample buffer. Immunoprecipitated proteins or whole cell lysates were separated by SDS-PAGE, transferred to 0.2 µm PVDF membrane (BioRad), blocked for 1 h in 10% non-fat milk at room temperature, probed for the protein of interest overnight at 4°C and visualized using HRP conjugated secondary antibodies (1:10,000) with the Immun-Star WesternC Chemiluminescence kit (BioRad). To determine which of the 3 Shc and Ras genes are expressed in Daoy-TrkA cells, 25 or 50 ug of whole cell lysates from Daoy-TrkA, Hela cells, E18 (brain), P3 (brain) or P20 mouse cortex were separated by either 10 or 12% SDS-PAGE and analysed as described above.

Confocal Microscopy. Daoy-TrkA cells were seeded (50,000 cells) and cultured on 35 mm glass bottomed dishes (MatTek Corporation) or poly D-lysine coated cover slips. When indicated, cells were transfected with the appropriate expression plasmid (1-2 µg) mixed with Lipofectamine 2000 (Life Technologies) in 100 µl of serum-free Optimem (Life Technologies) overnight or with a 1.5 ratio of Dreamfect Gold in 100 ul of serum-free Optimem for 4 hrs. Fresh media was provided and cells were either left untreated or treated with NGF as indicated. To monitor latex bead uptake, cells were plated on 35 mm glass bottom dishes and co-treated with 2 µl per ml of media with an aqueous suspension of fluorescent red (Excitation 575 nm; Emission 610 nm) labeled Latex beads (0.5 µm in diameter) (Sigma-Aldrich) and Alexa^{488}-Dextran (5 µg/ml; Life Technologies) or Alexa^{546}-transferrin (10 µg/ml; Life Technologies) and

Alexa^{488}-Dextran (5 µg/ml; Life Technologies) prior to stimulation with 100 ng/ml NGF. Cells were visualized and captured with a Zeiss 510 Meta laser scanning confocal microscope using a 63X oil objective (optical section width of 0.7 µm).

Trypan Blue Exclusion Assay. NGF-dependent cell death in Daoy-TrkA cells was quantified by trypan blue exclusion, 24 h following NGF stimulation. Cells were trypsinized, diluted 1:4 with 0.4 % trypan blue solution and the number of total cells and blue cells were counted by phase contrast microscopy on a hemacytometer. All experiments were performed in triplicate.

Statistical Analysis. All of the experiments were conducted at least three times. One way analysis of variance (ANOVA) with Tukey multiple comparison tests were used to analyse the difference of means among each groups. P value < 0.05 is considered statistically significant.

Results

TrkA generates large (0.5 µm) macropinosomes.

To determine whether TrkA induced macropinocytosis is distinct from receptor-mediated endocytosis we employed two reporters, namely, Alexa^{546}-transferrin as a probe for receptor-mediated endocytosis and Alexa^{488}-dextran as a general tracer of fluid uptake *via* any mechanism. In the absence of NGF, we find significant co-localization of Alexa^{488}-dextran and Alexa^{546}-transferrin consistent with dextran being co-internalized with transferrin *via* endocytosis; however, in the presence of NGF, the bulk of Alexa^{488}-dextran (green) internalizes independent of Alexa^{546}-transferrin (red) into large macropinosomes (Figure 1A). We then investigated the initial size of the vacuoles formed using Alexa^{546}-labeled latex beads and monitored their co-localization with Alexa^{488}-dextran. We found that cells could readily internalize 0.5 µm Alexa^{546}-latex beads in response to NGF and that this showed significant co-

252 localization with the Alexa^{488}-labeled dextran (Figure 1B). By comparison, cells were not able
253 to internalize 1.0 μm Alexa^{488}-latex beads (data not shown).

254 **Phosphatidylinositol 4-phosphate 5-kinase (PIP_5K) and phosphatidylinositol 3 (PI3) kinase**
255 **(PI3 kinase) participate in TrkA-induced macropinosome formation**

256 We then initiated a series of experiments to characterize both the composition of the TrkA-
257 induced macropinosome membranes as well as the signaling mechanism(s) that regulate their
258 growth. We first determined whether TrkA-induced macropinosome membranes contain
259 components identified in either constitutive or stimulated macropinosomes described in the
260 literature, specifically, phosphatidylinositol (4,5)-bisphosphate (PIP_2) and phosphatidylinositol
261 (3,4,5)-triphosphate (PIP_3) (15). We used EGFP tagged constructs encoding the PH domain of
262 AKT, which preferentially binds PIP_3 and to a lesser extent PIP_2, as well as the PH domain of
263 phospholipase D which only binds PIP_2 (31). Cells transfected with EGFP alone show diffuse
264 green staining throughout the cell and the macropinosome ruffles are not clearly identified
265 (Figure 1C); however, we found that both EGFP tagged PH domain constructs were present
266 within the macropinosome ruffles indicating that both PIP_2 and PIP_3 are components of the initial
267 lamellipodia (Figure 1C/D). In fact, some of the initial macropinosomes contained Alexa^{546}-
268 dextran (yellow arrows) used as a fluid tracer. However, as the vacuoles internalized from the
269 cell surface, both PH-AKT and PH-PLD were lost from the membrane, consistent with the fact
270 that both PIP_2 and PIP_3 are lost during endocytosis (15). Consistent with our observation that
271 NGF-dependent Alexa^{488}-dextran internalization was independent of receptor mediated
272 transferrin uptake (Figure 1A), we found that EGFP-tagged clathrin did not label TrkA-induced
273 macropinosomes (Figure 1E).
274

TrkA Stimulation causes Activation of H-Ras and Rac

To define TrkA-dependent pathways that drive macropinocytosis, we focused on molecules that serve roles in clathrin-independent endocytosis and macropinocytosis-dependent actin remodeling. Collectively, these include PAK1, PI3 kinase, Src (32), as well as several GTPases including H-Ras, Cdc42, Rac1, Rab5, Arf1, Arf6, RhoA and CtBP1/BARS (15);(16);(21);(33);(34);(35). With respect to Trk signaling, TrkA has been shown to activate H-Ras, Rap-1, Rac, Cdc42 as well as to negatively regulate RhoA, depending on the cellular context (36);(37);(38);(39);(40);(41);(42);(43);(44);(45). Thus, we first examined the NGF-induced activation kinetics of these GTPases using GST fusion proteins that contain binding domains of effector proteins that only bind the activated GTPases (PAK-1 for Rac and Cdc42, c-Raf-1 for H-Ras, Ral GDS for Rap1 and GGA3 for Arf6). Rac1 showed low basal activity in un-stimulated cells and was weakly activated, as early as 10 minutes, in response to NGF (Figure 2A). By comparison, there also were basal levels of H-Ras activation in un-stimulated cells; however, in response to NGF, we observed a larger increase in H-Ras activation as early as 10 minutes, which peaked at 6 h and remained elevated for up to about 12 h. Endogenous levels of H-Ras expression also remained constant during the 24 h period (Figure 2B). When we directly compared activation levels of H-Ras relative to Rac, we found that Ras activation ranges from 3 to 7-fold while activation of Rac is less than 1-fold (Figure 2C). By comparison, we found basal levels of Rap1, Cdc42 and Arf-6 activation in un-stimulated cells and while Arf6 has never been shown to be activated by TrkA, it is activated downstream of some RTKs such as the Met (46) and MUSK receptors (47) and it is involved in some forms of clathrin-independent endocytosis (15);(48). However, NGF did not stimulate any obvious change in the activation of Rap1, Cdc42 or Arf6 in Daoy-TrkA cells during the 24 h period of stimulation (Suppl. Fig 1).

298 To compliment the GTPase activation assays, we next determined whether dominant
299 negative (DN) GTPase expression affected NGF-dependent macropinocytosis and found that
300 DN-H-Ras and DN-Rab5 blocked NGF-induced macropinosomes, DN-Arf-6 reduced the
301 macropinosome size, while DN-Rap1b, Rab7, Rac1, Arf1, Rab34, Dyn-2, Cdc42 and
302 CtBP1/Bars had no effect (Figure 3A). While NGF did not affect basal levels of Arf6 activation
303 in Daoy-TrkA cells, the observation that DN-Arf6 reduced macropinosome size is consistent
304 with the literature, in that it traps activated H-Ras in recycling endosomes (49), and with our
305 observation that DN-Arf6 generated small macropinosomes containing Alexa^{546}-dextran (Figure
306 3A). The ability of DN-Rab5 to block NGF-induced macropinosomes is consistent with its
307 known roles in mediating the early fusion of endosomes (15) and H-Ras-induced
308 macropinosomes (49). With respect to DN-Rac1, as stated earlier, CA-Ras-dependent activation
309 of macropinocytosis in U251 cells increases the pool of active Rac1 (21),(23), which is known to
310 serve a role in membrane ruffling and the formation of lamellipodia (50),(51),(52). In contrast,
311 we found the levels of NGF-activated Rac1 in Daoy-TrkA cells were relatively low by 12-24 h
312 (Figure 2C), consistent with the fact that DN-Rac could not prevent TrkA-dependent
313 macropinocytosis and that pre-treatment of cells with the Rac specific inhibitor, EHT1864 (5
314 μM), did not block NGF-induced macropinosome formation despite its ability to block Rac1
315 activation at 6 h (Figure 3B).

316 In a complimentary approach, we then evaluated whether over-expression of constitutively
317 active (CA) GTPases could drive NGF-independent macropinocytosis in Daoy cells (Figure 4A).
318 We found that over-expression of both CA-Ras and CA-Arf6 caused the generation of large
319 vacuoles, consistent with macropinocytosis, CA-Rac1 generates small vacuoles while CA-
320 Cdc42, CA-Rab34 and CA-Rap1b did not generate any. Since NGF did not stimulate any

change in Arf-6 activation, the CA-Arf6 vacuoles likely represent trapped vacuoles that cannot recycle back up to the membrane and subsequently fuse (15). Collectively, these observations suggest that H-Ras is the primary GTPase driving TrkA-dependent macropinosome formation. To test this hypothesis further, we addressed whether CA-Ras induced macropinosomes could be blocked by the CK1 specific inhibitor, D4476 (53), which we previously found to block TrkA-induced macropinocytosis (13). As expected, we found that CA-Ras, but not CA-Arf6, induced macropinosomes could be completely blocked by D4476 (Figure 4B). We further examined the phospholipid composition (PIP_2, PIP_3) of CA-Arf6 and CA-Ras induced macropinosomes, compared to those induced by TrkA, by co-expressing EGFP-CA-Arf6 and CA-Ras with RFP-fused PH domains of AKT and PLD. We found that CA-Arf6 vacuoles contain both PIP_2/PIP_3 (Figure 4C) consistent with previous reports showing that unless Arf6 is inactivated shortly after the initial stage of membrane internalization, and PIP_2 is lost, that the vacuoles are trapped and become progressively larger as they fuse (54). In contrast, we found that while the initial CA-Ras-induced ruffles contained PIP_3, based on the co-staining with EGFP-PH-AKT (Figure 4D, yellow arrows), the internalized macropinosomes did not (Figure 4D, white arrows). By comparison, while all of the CA-Arf6 induced macropinosomes still contained PIP_2, only a few of the CA-Ras induced macropinosome contained PIP_2 (Figure 4D, white arrows). These observations are consistent with the lack of both AKT and PLD being localized to the large internal TrkA-induced macropinosomes (Figure 1C,D) and further support the model that H-Ras is the primary GTPase driving this process. Consistent with this logic, the EGFP-tagged Ras binding domain (RBD) and cysteine-rich domain (CRD) of the effector protein c-Raf-1 labeled both the initial membrane ruffles as well as the enlarged vacuolar membranes (Figure 4E, yellow

343 arrows). By comparison, an EGFP-tagged c-Raf-1 RBD-CRD mutant ($R^{89}A$), which can no
344 longer bind activate H-Ras, was diffusely distributed in the cell (Figure 4F) (55).

345 **Knockdown of H-Ras prevents TrkA-induced Macropinocytosis**

346 To control against potential off-target effects generated by over-expressing DN constructs,
347 we utilized siRNAs to deplete specific GTPases and assayed changes in NGF-induced
348 macropinocytosis. Transfection of siRNAs for both Cdc42 and Rac1 effectively decreased their
349 expression by 24 h relative to control siRNAs (Figure 5A). However, when Daoy-TrkA cells
350 were co-transfected with both siRNAs, along with a Cy3-labelled control siRNA to identify
351 transfected cells, there was no apparent decrease in the size of the NGF-induced $Alexa^{488}$-dextran
352 containing vacuoles relative to cells transfected with a control siRNA (Figure 5B). For Ras, we
353 first determined which of the 3 Ras genes (Harvey [H], Kirsten [K] and/or Neuroblastoma [N])
354 are expressed in Daoy-TrkA cells and found high levels of H-Ras and K-Ras compared to low
355 levels of N-Ras (Figure 5C). Given our over-expression studies with CA and DN-H-Ras, we
356 first determined how changes in H-Ras expression, alone, would affect NGF-induced
357 macropinosomes. Using an siRNA specific to H-Ras, we found that it effectively reduced
358 endogenous expression of H-Ras (Figure 5D) as well as the size of NGF-induced vacuoles in
359 Cy3 (red) positive co-transfected cells (Figure 5E) relative to cells transfected with siRNA
360 controls.

361 **The FRS2 Adapter, not ShcA, is Essential to TrkA-induced Macropinosome Formation**

362 NGF activation of TrkA results in receptor dimerization, phosphorylation of the activation
363 loop tyrosines, Tyr^{683}/Tyr^{684}, and subsequent phosphorylation of $Tyr^{490/499}$ in the juxtamembrane
364 region. This enables competitive binding between the Shc and FRS2 adapters to $pTyr^{490}$ (27)
365 and since both Shc and FRS2 are able to activate H-Ras (Figure 6A), we determined which

adapter is essential to this process. The Shc family of adapters includes 4 members (ShcA, B, C and D) (56). ShcA is highly expressed during embryogenesis and only expressed in progenitor cells in the mature brain while ShcB/C are primarily expressed after birth and ShcD is primarily expressed outside the nervous system. We first determined which Shc adapters were expressed in Daoy-TrkA cells, compared to lysates prepared from E18, P3 and P20 mouse cortices. We found that Daoy-TrkA cells only express ShcA (Figure 6B). Then we assayed FRS2/ShcA siRNAs for loss of expression in transfected Daoy-TrkA cells and found that both siRNAs effectively reduced expression of their target proteins, relative to a scrambled siRNA control (Figure 6B). Daoy-TrkA cells were then co-transfected with ShcA/FRS2 siRNAs, along with a Cy3-labelled siRNA control, and Cy3 positive cells were examined for changes in Alexa^{488}-dextran uptake relative to cells transfected with control siRNA (LC3). Accordingly, we found that loss of FRS2, but not ShcA, effectively reduced the size of NGF-induced macropinosomes comparable to those observed in un-stimulated cells (Figure 6C).

Src Kinase is Essential to NGF-induced Macropinosome Formation

The soluble tyrosine kinase, Src, is another candidate signaling molecule that has been shown to be involved in membrane ruffling and macropinocytosis in different cellular contexts (32)[,](57)[,](58). Although the molecular mechanisms involved in Src mediated macropinocytosis have not been fully elaborated, many of the pathways involve several downstream effectors such as PI3 kinase, phospholipase C as well as phospholipase D (15). Importantly, Src is known to be involved in TrkA-dependent signaling. Specifically, Src activation precedes the activation of H-Ras and it is recruited into TrkA signaling *via* FRS2 (Figure 7A) (26)[,](27)[,](59). In our initial studies to investigate whether Src was involved in NGF-induced macropinocytosis, we determined whether the Src inhibitor, PP2, affected the process. Interestingly, we found that 7.5

389 μM PP2 effectively reduced macropinocytosis to levels observed with vehicle alone (Figure 7B)
390 and that this concentration did not affect TrkA kinase activity (Figure 7C). While higher
391 concentrations of PP2 also blocked cell death, they impeded NGF-induced phosphorylation of
392 the juxtamembrane pTyr^{490} residue (Figure 7C). Activation of Src involves the de-
393 phosphorylation of the self-inhibitory carboxyl-terminal tyrosine residue, Y^{527}, and
394 phosphorylation of Y^{416} which resides in the activation loop (60)-(61)-(62). When we examined
395 the kinetics of Src phosphorylation in response to NGF in Daoy-TrkA cells, we observed a
396 significant increase in the amount of phosphorylation at Y^{416} by 6 h, which subsequently decayed
397 over time (Figure 7D), with little change in the phosphorylation state of Y^{527} (data not shown).
398 Co-treatment with the CK1 inhibitor, D4476, did not affect the kinetics of Src activation (Figure
399 7D; right panel) indicating that CK1 activation is either independent or downstream of Src. We
400 then used siRNAs to address the role of Src expression/activation on NGF-induced
401 macropinocytosis. A Src siRNA effectively reduced Src expression by 24 h and this remained
402 reduced up to 72 h post transfection (Figure 7E). Moreover, we found that cells co-transfected
403 with Src siRNA plus a Cy3-labelled control siRNA showed a large reduction in the
404 internalization of Alexa^{488}-dextran compared to cells transfected with control siRNAs and, in
405 fact, internalized Alexa^{488}-dextran to levels similar to un-stimulated cells (Figure 7F). Finally,
406 we expressed EGFP tagged wild type Src, as well as a DN-Src mutant (1-516) (32), in Daoy-
407 TrkA cells and determined how their expression affected NGF-induced macropinocytosis. The
408 results demonstrate that over-expression of wt-Src does localize to large macropinosomes in
409 NGF-stimulated cells (Figure 7G). In contrast, over-expression of DN-Src-GFP effectively
410 blocks NGF-induced macropinosome formation (Figure 7G).
411

Casein Kinase 1 phosphorylation and Inactivation of RhoB facilitates Macropinocytosis.

We next addressed the role of RhoB, another member of the Rho family of small GTPases which also includes RhoA and RhoC in macropinocytosis (63). RhoB is involved in a variety of cellular functions including the organization and maintenance of actin stress fibers (64). Thus, we first analyzed cells for NGF-dependent changes in the activation of RhoB using a GST fusion construct encoding the Rho binding domain of the effector protein Rhotekin. In contrast to all the other GTPases tested (Figure 2, Supplementary Figure 1), we found a steady decrease in both the activation and expression levels of RhoB in response to NGF such that by 12 h, the amount of active RhoB was approximately half that observed at 6 h (Figure 8A). In fact, no active RhoB was observed by 24 h, though its levels of expression remained constant between 12-24 h (Figure 8A). We then addressed whether inactivation of RhoB was essential to macropinosome formation and found that expression of CA-RhoB ($Q^{63}L$,) and the maintenance of actin stress fibers, effectively blocked NGF-induced macropinocytosis (Figure 8B).

Previously, we showed that the CK1 inhibitor D4476 completely blocked NGF-induced macropinocytosis in Daoy-TrkA cells, although the mechanism was not initially clear (13). However, Tillement, *et al.* demonstrated that RhoB, but neither RhoA nor RhoC, is a direct target of CK1δ kinase activity *in vitro* (28). Specifically, they demonstrated that RhoB is phosphorylated at Ser^{185} and this results in the inactivation of RhoB (28). Thus, we considered the possibility that the failure to inactivate RhoB, and the maintenance of actin stress fibers, underscores the inhibitory action of D4476. To address this, we examined how expression of a RhoB $S^{185}A$ mutant affects NGF-induced macropinocytosis. As this mutant is incapable of being phosphorylated at Ser^{185}, it should exert a similar effect as CA-RhoB ($Q^{63}L$) and block NGF-induced macropinosome formation. Consistent with this logic, we found that expression of the

435 RhoB ($S^{185}A$) mutant did, in fact, completely block NGF-induced macropinocytosis (Figure 8B).
436 To compliment these studies, we reduced RhoB expression, by RNA siRNA transfection, and
437 observed enhanced macropinocytosis in response to NGF indicating that loss of RhoB dependent
438 stress fibres are essential (Figure 8C).

439 **RhoA Activation is Essential to NGF-induced Macropinosome Formation**

440 We have demonstrated that the primary GTPase driving NGF-induced macropinocytosis
441 in Daoy-TrkA cells is H-Ras (Figures 2-5). However, activation of H-Ras, itself, does not
442 directly affect F-actin re-organization. Thus, we considered whether activation of RhoA, which
443 is known to directly affect F-actin re-organization, was activated by NGF in Daoy-TrkA cells,
444 whether it was localized to the macropinosome membranes and whether it was essential to drive
445 macropinocytosis. In this respect, RhoA activation has been shown to be associated with both
446 neurite/dendritic extension and retraction in the nervous system (65);(66);(67);(68);(40);(69). We
447 examined the kinetics of NGF-induced activation of RhoA in Daoy-TrkA cells, using a GST
448 fusion protein containing the Rho binding domain of Rhotekin, and observed RhoA activation as
449 early as 10 min in response to NGF, peak activation at 6 h and while the abundance of RhoA
450 decreased by 12-24 h, the remaining molecules were still active (Figure 9A). Next, we used a
451 GFP-tagged reporter construct to visualize active RhoA (GFP-rGBD) and found that RhoA is
452 diffusely distributed within the cytoplasm of un-stimulated cells; however, following NGF
453 stimulation, RhoA localized to the lamellpodia that are initiating macropinocytosis, suggesting
454 that it is the final GTPase stimulating F-actin re-organization (Figure 9B). To confirm that RhoA
455 activation is essential to NGF-induced macropinocytosis, we transfected Daoy-TrkA cells with
456 YFP-tagged DN-RhoA ($T^{19}N$) and observed that it effectively blocked NGF-induced uptake of
457 $Alexa^{546}$-dextran (Figure 9C). Moreover, NGF-induced macropinosomes were effectively

458 blocked by the Rho inhibitor, CT04 (Fig 9D). Collectively, these data confirmed that RhoA is
459 the final GTPase regulating actin re-organization and macropinosome formation in response to
460 NGF stimulation of Daoy-TrkA cells.

461 **Discussion**

462 We previously demonstrated that TrkA expressing Daoy cells undergo NGF-dependent
463 macropinocytosis resulting in cell death (13). Here, we have characterized the essential
464 signaling cascade that drives this process. Specifically, it involves the recruitment of the FRS2
465 adaptor to activated TrkA and the subsequent activation of Src, H-Ras, RhoA and the CK1-
466 dependent inactivation of RhoB (Figure 10). We found that macropinosomes are generated
467 independently of receptor-mediated internalization, do not contain clathrin, and can be as large
468 as 0.5 μm in size (Figure 1). NGF-dependent cell death in Daoy-TrkA cells was strikingly
469 similar to that observed in the Gb cell line U251 following expression of activated H-Ras
470 (20)[,](21)[,](23). Similar to U251 cells, macropinocytosis in Daoy-TrkA cells is also dependent on
471 the activation of H-Ras. Specifically, expression of DN-H-Ras (Figure 3) and/or H-Ras siRNAs
472 (Figure 5D/E) completely blocked NGF-induced macropinocytosis. Conversely,
473 macropinocytosis was induced in the absence of NGF by expression of CA-H-Ras (Figure 4A)
474 and CA-H-Ras induced macropinosomes could be blocked with the CK1 inhibitor, D4476
475 (Figure 4B), that blocks NGF-induced macropinosomes (13). Finally, a construct encoding the
476 Ras binding domain of c-Raf-1 (RBD-CRD) clearly demonstrated that active H-Ras was
477 localized to the macropinosome membranes (Figure 4E) as compared to the diffuse staining
478 throughout the cytosol observed with the EGFP-tagged c-Raf-1 RBD-CRD mutant ($R^{89}A$) that
479 cannot bind activated H-Ras (Figure 4F) (55). Collectively, these data all support the conclusion
480 that H-Ras is the primary TrkA-coupled GTPase driving macropinocytosis. While H-Ras could

be activated, *via* either Shc or FRS2, which compete for receptor binding following phosphorylation of the juxtamembrane tyrosine residue Y^{490} on TrkA (27) (Figure 10), our studies demonstrate that FRS2 is the TrkA-dependent adapter essential to the process. Specifically, loss of FRS2, but not ShcA, expression prevents NGF-induced macropinocytosis (Figure 6). While activation of H-Ras is commonly associated with tumor cell growth and many carcinomas arise as a result of mutations in H-Ras, it is important to note that activation of H-Ras has never been reported as a cancer causing oncogene in human brain tumors (24)(25). H-Ras has been shown to have a diversity of roles in different cell types including inducing macropinocytosis to facilitate nutrient uptake in pancreatic tumors (14) in addition to its well known roles in regulating cell survival (70), senescence (71) and cell death (72). As described earlier, H-Ras has been shown to stimulate macropinocytosis in U251 cells, *via* activation of Rac1 (23), and expression of CA-Rac1 can itself stimulate macropinocytosis and cell death (21). This is in contrast to our observations where expression of CA-Rac1 had no effect on macropinosome formation and the expression of DN-Rac1 and/or depletion of endogenous Rac1 by siRNA did not affect NGF-induced macropinocytosis. Moreover, while NGF induced a rapid increase in activated Rac1 that was sustained up to approx. 12 h, the increase in activation was less than 1-fold as compared to the 3 to 7-fold increase in H-Ras activation during the same time period (Figure 2C). While Rac1 is rapidly activated in response to NGF in PC12 cells, and it is necessary for Rho inactivation and the release of stress fibers to facilitate neurite outgrowth (44), we found that Rac1 activation was not essential for NGF-dependent macropinocytosis in Daoy-TrkA cells. In fact, the Rac-specific inhibitor, EHT 1864, had no effect on NGF-induced macropinocytosis, despite effectively blocking Rac activity (Figure 3B).

503 Another small GTPase implicated in macropinocytosis and modulating actin dynamics and
504 endosomal recycling required for some types of clathrin-dependent and clathrin-independent
505 endocytosis is Arf6 (73)·(15)·(48). Arf6 resides at the plasma membrane and when activated
506 stimulates the accumulation of PIP_2 at the membrane through activation of phosphatidylinositol
507 4-phosphate 5 kinase (PIP_5K) and phospholipase D (PLD) (54)·(74)·(75) resulting in changes in
508 the actin cytoskeleton (76). Following internalization of the endosome or macropinosome, Arf6
509 is inactivated and PIP_2 is lost from the endosomal membrane (54) to be replaced by PIP_3 (49) by
510 PI3 kinase (77). Under normal conditions where the macropinosome matures and is then
511 recycled back up to the cell membrane, activation of Arf6 is again required for this final step and
512 membrane fusion (54)·(78). In U251 cells, the resting activity of Arf6 is high but drops
513 significantly upon stimulation of macropinocytosis (23). In contrast to these results, we
514 observed no change in the activation levels of Arf6 in NGF-stimulated Daoy-TrkA cells.

515 As has been observed in other cells (54)·(49), expression of CA-Arf6 induced massive
516 vacuolization similar to that observed with CA-H-Ras in Daoy-TrkA cells. However, the
517 phosphatidylinositide composition of the CA-Arf6 induced macropinosomes are different from
518 those induced by both NGF (Figure 1) and CA-H-Ras (Figure 4) in that CA-Arf6 induced
519 macropinosomes result from the continual fusion of primary vacuoles due to the continued
520 activation of PIP_5K and PLD (54)·(15) and, as such, are enriched in PIP_2 and PIP_3 (15)·(48)·(54).

521 Many of the proteins involved in macropinocytosis are downstream effectors of the non-
522 receptor tyrosine kinase Src. In fact, expression of CA-Src can induce the formation of
523 membrane ruffles and macropinosomes in various cell types including COS-7, HeLa, MDCK
524 and mouse embryonic fibroblasts (MEF cells) (58)·(32)·(79) and also induces rapid loss of actin
525 stress fibers in MEF's (80). In addition, active Src associates with macropinosomes, and remains

associated through maturation up to fusion with lysosomes (32). We found that inhibition of Src by PP2 (7.5 μm) resulted in a reduction of macropinocytotic cell death in NGF-treated Daoy-TrkA cells, comparable to control levels, without affecting TrkA phosphorylation (Figure 7B/C). Similarly, siRNA mediated knock down of Src led to a reduction in vacuole formation in the presence of NGF, comparable to that of controls (Figure 7E/F). In fact, over-expressing WT-Src led to larger NGF-induced macropinosomes in Daoy-TrkA cells and Src was clearly localized on the internalized vacuoles, while expression of a DN mutant effectively blocked NGF-dependent macropinosomes (Figure 7G). Src activation precedes the activation of H-Ras, is necessary for the sustained activation of Erk1/2 essential to neurite outgrowth in PC12 cells (81)[,](82)[,](83), and it is recruited into TrkA signaling *via* FRS2 (27) (Figure 10).

The final steps in driving macropinocytosis requires membrane ruffling and lamellipodia formation that are dependent upon the relaxation of actin stress fibers, which enables actin to be remodeled (15)[,](16). Members of the Rho family of GTPases, in particular Rho A, B and C, have been shown to play important roles in the organization and maintenance of actin stress fibers (84). Our data indicates that relaxation of actin stress fibers, by CK1-dependent phosphorylation and inactivation of RhoB, at residue Ser^{185}, is an essential initial requirement in the induction of macropinocytosis. How TrkA regulates the constitutive kinase activity of CK1 (85) and drives the phosphorylation of RhoB, downstream of H-Ras, remains to be clarified. In contrast, we found that activation of the related Rho family GTPase, RhoA, is essential to stimulate the actin re-organization and lamellipodial formation required to generate macropinosomes (Figure 10). While RhoA has classically been thought to only regulate stress fiber formation, using FRET based reporters, Kurokawa and Matsuda demonstrated that RhoA is also highly activated in membrane ruffles and nascent lamellipodia in multiple cell lines in

549 response to different stimuli (86). Using a GST fusion protein containing the Rho binding
550 domain of Rhotekin, we found RhoA highly activated in response to NGF, with peak activation
551 at 6 h, and lower levels of activation by 12-24 h (Figure 9A). By using a reporter construct
552 encoding the Rho binding domain of Rhoteckin to visualize active RhoA (GFP-rGBD), we found
553 that active RhoA was diffusely distributed within the cytosol of un-stimulated Daoy-TrkA cells
554 but in response to NGF, RhoA localized to the membrane ruffles and lamellipodia (Figure 9B,
555 yellow arrows). Moreover, we found that expressing YFP-tagged DN-RhoA ($T^{19}N$) (Figure 9C)
556 as well treating Daoy-TrkA cells with the Rho inhibitor, CT04 (Figure 9D), effectively blocked
557 NGF-induced macropinocytosis.

558 In summary, we have shown that macropinocytosis in Daoy-TrkA cells can be stimulated in
559 the absence of NGF by expression of a CA mutant of H-Ras ($G^{12}V$). In addition, NGF-induced
560 macropinocytosis is prevented in cells expressing a DN-H-Ras mutant ($T^{17}N$). In contrast to
561 glioblastoma U251 cells, we see no induction of macropinocytosis with a CA-Rac1 mutant
562 ($Q^{61}L$) and conversely no protection against NGF induced macropinocytosis in the presence of
563 DN-Rac1 ($T^{17}N$). Other small GTPases such as Cdc42, while activated by the addition of NGF,
564 do not appear to be essential in the initiation of macropinocytosis in Daoy-TrkA cells. Finally,
565 inactivation of RhoB by phosphorylation at Ser^{185} by CK1 is fundamentally important in the
566 induction of NGF-induced macropinocytosis. Inactivation of RhoB relaxes actin stress fibers
567 and allows for actin remodeling, the formation of membrane ruffles and lamellipodia.
568 Conversely, activation of RhoA is the final and essential GTPase that re-organizes actin and
569 generates the macropinosomes.

570 Considering the potential impact of these data, Vander Heiden *et al*. have reviewed the
571 literature and discussed the fact that exploiting the Warburg effect, the reliance of most cancer

572 cells on aerobic glycolysis and their need for large quantities of external nutrients to support
573 biomass production, has been proposed as a general strategy to selectively kill cancer cells (87).
574 Recently, for example, Yun *et al*. have demonstrated that colorectal cancer cells expressing K-
575 RAS and B-RAF oncogenic mutants are selectively sensitive to high concentrations of vitamin C
576 due to the over-expression of a glucose transporter GLUT1 in these cells, which takes up de-
577 hydroascorbic acid, ultimately causing accumulation of reactive oxygen species and cell death
578 (88). Thus, the otherwise advantageous ability to uptake more glucose actually makes these cells
579 more susceptible to cell death. Macropinocytosis is a normal cellular process by which cells
580 internalize extracellular fluids and nutrients from their environment and is one strategy that Ras-
581 transformed cancer cells use to increase uptake of amino acids to meet the needs of rapid growth
582 (14); but, we have found that non-Ras transformed medulloblastomas become susceptible to a
583 TrkA-driven Ras-dependent uncontrolled macropinocytosis and tumor cell death (13). The links
584 our studies provide here between TrkA and the regulation of GTPases and the resulting effects
585 on actin cytoskeletal dynamics now provides the basis to test therapeutic strategies that target
586 these pathways.
587

588 **Author Contributions.** SOM conceived and supervised the project. CL performed confocal
589 microscopy, cell culture, biochemical experiments and data analyses. JL, AT and JISM
590 performed cell culture, biochemical experiments and data analyses. CS perfomed confocal
591 studies. SHP and SWM provided essential reagents and intellectual support.
592
593 **Conflicts of Interest.** The authors declare that they have no conflict of interest.
594
595 **Acknowledgements.** The authors would like to thank the many investigators who provided
596 constructs for the experiments described herein; specifically GST-GGA3 (M. Park, McGill
597 University, Montreal), GST-RhoRBD, DN and CA RhoB (Dr. A. Richmond, Vanderbilt Univ.,
598 TN), GST-PAK-CRIB (Dr. A. Hall, Sloane-Kettering, NY), GST-Ras RBD (Dr. D. Shalloway,
599 UC Berkeley, CA), PH domains of AKT and PLCδ as well as the RBD-CRD domains of c-Raf-
600 1 fused with EGFP (Dr. T. Balla, NIH, MD), the CRD c-Raf-1 $R^{89}A$ mutant (Dr. Y. Sako,
601 RIKEN ASI, Japan), DN and CA-Arf6 (Dr. J. Donaldson, NIH, MD), DN and CA-Rap1b (Dr. P.
602 Stork, Vollum Inst, OR), WT and DN Src (Dr. N. Yamaguchi, Chiba Univ., Japan), CA ($G^{12}V$)
603 and DN ($T^{17}N$) Cdc42, DN ($S^{17}N$) Rac, DN ($K^{44}A$) Dynamin 2, DN ($T^{31}N$) Arf1, DN ($N^{19}L$)
604 RhoA, DN ($S^{34}N$) Rab5, DN ($T^{22}N$) Rab7 and EGFP- tagged Clathrin (Dr. S. Ferguson, Univ.
605 Ottawa, On, CA); DN ($S^{147}A$) CtBP1/BARS (Alberto Luini, Institute of Protein Biochemistry,
606 Naples, Italy); DN ($T^{66}N$) and CA ($Q^{111}L$) Rab34 (Dr. T. Endo, Chiba University, Chiba, Japan)
607 and the RhoB ($S^{185}A$) mutant (Dr. A. Pradines, INSERM, France). This research was supported
608 with funds from an operating grant from the Cancer Research Society Inc. to SOM, the Canadian
609 Institutes of Health Research to SWM (MOP-GMX-93643) as well as from private donations.
610

611 **References**

612 1. **Kim JY, Sutton ME, Lu DJ, Cho TA, Goumnerova LC, Goritchenko L, Kaufman**
613 **JR, Lam KK, Billet AL, Tarbell NJ, Wu J, Allen JC, Stiles CD, Segal RA and Pomeroy SL**.
614 1999. Activation of neurotrophin-3 receptor TrkC induces apoptosis in medulloblastomas.
615 Cancer Res **59**: 711-719.
616 2. **Brodeur GM**. 2003. Neuroblastoma: biological insights into a clinical enigma. Natue
617 Rev. Cancer **3**: 203-216.
618 3. **Marino S**. 2005. Medulloblastoma: developmental mechanisms out of control. Trends
619 Mol Med **11**: 17-22.
620 4. Nakagawara A: Neural crest development and neuroblastoma: the genetic and biological
621 link. In: Luigi A and Laura C (eds). Progress in Brain Research. Elsevier, 2004, pp 231-242.
622 5. **Brodeur GM, Minturn JE, Ho R, Simpson AM, Iyer R, Varela CR, Light JE, Kolla**
623 **V and Evans AE**. 2009. Trk Receptor Expression and Inhibition in Neuroblastomas. Clinical
624 Cancer Research **15**: 3244-3250. 10.1158/1078-0432.ccr-08-1815
625 6. **Gulino A, Arcella A and Giangaspero F**. 2008. Pathological and molecular
626 heterogeneity of medulloblastoma. Current Opinion in Oncology **20**: 668-675
627 7. **Harel L, Costa B and Fainzilber M**. 2010. On the death Trk. Developmental
628 Neurobiology **70**: 298-303. 10.1002/dneu.20769
629 8. **Thomaz A, Jaeger M, Buendia M, Bambini-Junior V, Gregianin LJ, Brunetto AL,**
630 **Brunetto AT, de Farias CB and Roesler R**. 2015. BDNF/TrkB Signaling as a Potential Novel
631 Target in Pediatric Brain Tumors: Anticancer Activity of Selective TrkB Inhibition in
632 Medulloblastoma Cells. Journal of Molecular Neuroscience: 1-8. 10.1007/s12031-015-0689-0
633 9. **Chou TT, Trojanowski JQ and Lee VM**. 2000. A novel apoptotic pathway induced by
634 nerve growth factor-mediated TrkA activation in medulloblastoma. J Biol Chem **275**: 565-570.
635 10. **Lavoie JF, LeSauteur L, Kohn J, Wong J, Furtoss O, Thiele CJ, Miller FD and**
636 **Kaplan DR**. 2005. TrkA Induces Apoptosis of Neuroblastoma Cells and Does So via a p53-
637 dependent Mechanism. J. Biol. Chem. **280**: 29199-29207.
638 11. **Jung EJ and Kim DR**. 2008. Apoptotic cell death in TrkA-overexpressing cells: kinetic
639 regulationof ERK phosphorylation and caspase-7 activation. Mol. Cells **26**: 12-17.
640 12. **Harel L, Costa B, Tcherpakov M, Zapatka M, Oberthuer A, Hansford LM,**
641 **Vojvodic M, Levy Z, Chen Z-Y, Lee FS, S.Avigad, Yaniv I, Shi L, Eils R, Fischer M, Brors**
642 **B, Kaplan DR and Fainzilber M**. 2009. CCM2 Mediates Death Signaling by the TrkA
643 Receptor Tyrosine Kinase. Neuron **63**: 585-591.
644 13. **Li C, MacDonald JIS, Hryciw T and Meakin SO**. 2010. Nerve Growth Factor
645 Activation of the TrkA Receptor induces Cell Death, by Macropinocytosis, in Medulloblastoma
646 Daoy Cells. J. Neurochem. **112**: 882-889.
647 14. **Commisso C, Davidson SM, Soydaner-Azeloglu RG, Parker SJ, Kamphorst JJ,**
648 **Hackett S, Grabocka E, Nofal M, Drebin JA, Thompson CB, Rabinowitz JD, Metallo CM,**
649 **Vander Heiden MG and Bar-Sagi D**. 2013. Macropinocytosis of protein is an amino acid
650 supply route in Ras-transformed cells. Nature **497**: 633-637.
651
652 15. **Donaldson JG, Porat-Shliom N and Cohen LA**. 2009. Clathrin-independent
653 endocytosis: A unique platform for cell signaling and PM remodeling. Cellular Signalling **21**: 1-
654 6.

16. **Lim JP and Gleeson PA**. 2011. Macropinocytosis: an endocytic pathway for internalising large gulps. Immunol Cell Biol **89**: 836-843.
17. **Lim J, Wang J, Kerr M, Teasdale R and Gleeson P**. 2008. A role for SNX5 in the regulation of macropinocytosis. BMC Cell Biology **9**: 58.
18. **Swanson JA and Watts C**. 1995. Macropinocytosis. Trends in Cell Biology **5**: 424-428. 10.1016/s0962-8924(00)89101-1
19. **Chi S, Kitanaka C, Noguchi K, Mochizuki T, Nagashima Y, Shirouzu M, Fujita H, Yoshida M, Chen W, Asai A, Himeno M, Yokoyama S and Kuchino Y**. 1999. Oncogenic Ras triggers cell suicide through the activation of a caspase-independent cell death program in human cancer cells. Oncogene **18**: 2281-2290.
20. **Kaul A, Overmeyer JH and Maltese WA**. 2007. Activated Ras induces cytoplasmic vacuolation and non-apoptotic death in glioblastoma cells via novel effector pathways. Cellular Signalling **19**: 1034-1043.
21. **Overmeyer JH, .Kaul A, Johnson EE and Maltese WA**. 2008. Active Ras Triggers Death in Glioblastoma Cells through Hyperstimulation of Macropinocytosis. Mol. Cancer Res. **6**: 965-977.
22. **Overmeyer J, Young A, Bhanot H and Maltese W**. 2011. A chalcone-related small molecule that induces methuosis, a novel form of non-apoptotic cell death, in glioblastoma cells. Molecular Cancer **10**: 69.
23. **Bhanot H, Young AM, Overmeyer JH and Maltese WA**. 2010. Induction of Nonapoptotic Cell Death by Activated Ras Requires Inverse Regulation of Rac1 and Arf6. Mol Canc Res. **8**: 1358-1374.
24. **FernÃ¡ndez-Medarde A and Santos E**. 2011. Ras in Cancer and Developmental Diseases. Genes & Cancer **2**: 344-358. 10.1177/1947601911411084
25. **Parsons DW, Li M, Zhang X, Jones Sn, Leary RJ, Lin JC-H, Boca SM, Carter H, Samayoa J, Bettegowda C, Gallia GL, Jallo GI, Binder ZA, Nikolsky Y, Hartigan J, Smith DR, Gerhard DS, Fults DW, VandenBerg S, Berger MS, Marie SKN, Shinjo SMO, Clara C, Phillips PC, Minturn JE, Biegel JA, Judkins AR, Resnick AC, Storm PB, Curran T, He Y, Rasheed BA, Friedman HS, Keir ST, McLendon R, Northcott PA, Taylor MD, Burger PC, Riggins GJ, Karchin R, Parmigiani G, Bigner DD, Yan H, Papadopoulos N, Vogelstein B, Kinzler KW and Velculescu VE**. 2011. The Genetic Landscape of the Childhood Cancer Medulloblastoma. Science **331**: 435-439. 10.1126/science.1198056
26. **Kremer NE, D'Arcangelo G, Thomas SM, DeMarco M, Brugge JS and Halegoua S**. 1991. Signal transduction by nerve growth factor and fibroblast growth factor in PC12 cells requires a sequence of src and ras. J. Cell. Biol. **115**: 809-819.
27. **Meakin SO, MacDonald JIS, Gryz EA, Kubu CJ and Verdi JM**. 1999. The Signaling Adapter Protein FRS-2 Competes with Shc for binding to TrkA: A Model for Discriminating Proliferation and Differentiation. J. Biol. Chem. **274**: 9861-9870.
28. **Tillement V, Lajoie-Mazenc I, Casanova A, Froment C, Penary M, Tovar D, Marquez R, Monsarrat B, Favre G and Pradines A**. 2008. Phosphorylation of RhoB by CK1 impedes actin stress fiber organization and epidermal growth factor receptor stabilization. Exp. Cell Res. **314**: 2811-2821.
29. **Boukerche H, Su Z, Prévot C, Sarkar D and Fisher PB**. 2008. mda-9/Syntenin promotes metastasis in human melanoma cells by activating c-Src. Proc Natl Acad Sci U S A **105**: 15914-15919.

30. **Deroanne CF, Hamelryckx D, Ho TTG, Lambert CA, Catroux P, Lapière CM and Nusgens BV**. 2005. Cdc42 downregulates MMP-1 expression by inhibiting the ERK1/2 pathway. Journal of Cell Science **118**: 1173-1183. 10.1242/jcs.01707
31. **Kutateladze TG**. 2010. Translation of the phosphoinositide code by PI effectors. Nat Chem Biol **6**: 507-513.
32. **Kasahara K, Nakayama Y, Sato I, Ikeda K, Hoshino M, Endo T and Yamaguchi N**. 2007. Role of Src-family kinases in Formation and Trafficking of Macropinosomes. J. Cell Physiol. **211**: 220-232.
33. **Liberali P, Kakkonen E, Turacchio G, Valente C, Spaar A, Perinetti G, Böckmann RA, Corda D, Colanzi A, Marjomaki V and Luini A**. 2008. The closure of PAK1-dependent macropinosomes requires the phosphoryation of CtBP1/BARS. The EMBO Journal **27**: 970-981.
34. **Swanson JA**. 2008. Shaping cups into phagosomes and macropinosomes. Nat. Rev. Mol. Cell. Biol. **9**: 639-649.
35. **Doherty GJ and McMahon HT**. 2009. Mechanisms of Endocytosis. Annu. Rev. Biochem. **78**: 857-902.
36. **Talebian A, Robinson-Brookes K, MacDonald JIS and Meakin SO**. 2013. Ras Guanine Nucleotide Releasing Factor 1 (RasGrf1) enhancement of Trk Receptor mediated Neurite Outgrowth requires Activation of both H-Ras and Rac. J. Mol. Neurosci. **49**: 38-51.
37. **Valdez G, Akmentin W, Philippidou P, Kuruvilla R, Ginty DD and Halegoua S**. 2005. Pincher-Mediated Macroendocytosis Underlies Retrograde Signaling by Neurotrophin Receptors. J. Neurosci. **25**: 5236-5247. 10.1523/jneurosci.5104-04.2005
38. **Chakrabarti K, Lin R, Schiller NI, Wang Y, Koubi D, Fan Y-X, Rudkin BB, Johnson GR and Schiller MR**. 2005. Critical Role for Kalirin in Nerve Growth Factor Signaling through TrkA. Mol. Cell. Biol. **25**: 5106-5118. 10.1128/mcb.25.12.5106-5118.2005
39. **York RD, Yao H, Dillon T, Ellig CL, Eckert SP, McClecksy EW and Stork PJ**. 1998. Rap1 mediates sustained MAP kinase activation induced by nerve growth factor. Nature **392**: 622-626.
40. **Jeon C-Y, Moon M-Y, Kim J-H, Kim H-J, Kim J-G, Li Y, Jin J-K, Kim P-H, Kim H-C, Meier KE, Kim Y-S and Park J-B**. 2012. Control of neurite outgrowth by RhoA inactivation. Journal of Neurochemistry **120**: 684-698. 10.1111/j.1471-4159.2011.07564.x
41. **Aoki K, Nakamura T and Matsuda M**. 2004. Spatio-temporal Regulation of Rac1 and Cdc42 Activity during Nerve Growth Factor-induced Neurite Outgrowth in PC12 Cells. J. Biol. Chem. **279**: 713-719. 10.1074/jbc.M306382200
42. **Ahmed I, Calle Y, Iwashita S and Nur-E-Kamal A**. 2006. Role of Cdc42 in neurite outgrowth of PC12 cells and cerebellar granule neurons. Molecular and Cellular Biochemistry **281**: 17-25. 10.1007/s11010-006-0165-9
43. **Kozma R, Sarner S, Ahmed S and Lim L**. 1997. Rho family GTPases and neuronal growth cone remodelling: relationship between increased complexity induced by Cdc42Hs, Rac1, and acetylcholine and collapse induced by RhoA and lysophosphatidic acid. Mol. Cell. Biol. **17**: 1201-1211.
44. **Nusser N, Gosmanova E, Zheng Y and Tigyi G**. 2002. Nerve Growth Factor Signals through TrkA, Phosphatidylinositol 3-Kinase, and Rac1 to Inactivate RhoA during the Initiation of Neuronal Differentiation of PC12 Cells. Journal of Biological Chemistry **277**: 35840-35846. 10.1074/jbc.M203617200
45. **Nakamura T, Komiya M, Sone K, Hirose F, Gotoh N, Morii H, Ohta Y and Mori M**. 2002. Grit, a GTPase-activating protein for the Rho family, regulates neurite extension through

association with the TrkA receptor and N-Shc and CrkL/Crk adapter molecules. Mol. Cell. Biol. **22**: 8721-8734.

46. **Parachoniak Christine A, Luo Y, Abella Jasmine V, Keen James H and Park M**. 2011. GGA3 Functions as a Switch to Promote Met Receptor Recycling, Essential for Sustained ERK and Cell Migration. Developmental Cell **20**: 751-763. http://dx.doi.org/10.1016/j.devcel.2011.05.007

47. **Luiskandl S, Woller B, Schlauf M, Schmid JA and Herbst R**. 2013. Endosomal trafficking of the receptor tyrosine kinase MuSK proceeds via clathrin-dependent pathways, Arf6 and actin. FEBS Journal **280**: 3281-3297. 10.1111/febs.12309

48. **Donaldson JG and Jackson CL**. 2011. ARF family G proteins and their regulators: roles in membrane transport, development and disease. Nat Rev Mol Cell Biol **12**: 362-375.

49. **Porat-Shliom N, Kloog Y and Donaldson JG**. 2008. A Unique Platform for H-Ras Signaling Involving Clathrin-independent Endocytosis. Mol. Biol. Cell **19**: 765-775. 10.1091/mbc.E07-08-0841

50. **Ridley AJ**. 2001. Rho family proteins: coordinating cell responses. Trends in Cell Biology **11**: 471-477. 10.1016/s0962-8924(01)02153-5

51. **Doughman RL, Firestone AJ, Wojtasiak ML, Bunce MW and Anderson RA**. 2003. Membrane Ruffling Requires Coordination between Type Iα Phosphatidylinositol Phosphate Kinase and Rac Signaling. Journal of Biological Chemistry **278**: 23036-23045. 10.1074/jbc.M211397200

52. **Wells CM, Walmsley M, Ooi S, Tybulewicz V and Ridley AJ**. 2004. Rac1-deficient macrophages exhibit defects in cell spreading and membrane ruffling but not migration. Journal of Cell Science **117**: 1259-1268. 10.1242/jcs.00997

53. **Bain J, Plater L, Elliott M, Shpiro N, Hastie CJ, McLauchlan H, Klevernic I, Arthur JSC, Aless DR and Cohen P**. 2007. The selectivity of protein kinase inhibitors: a further uptake. Biochem. J. **408**: 297-315.

54. **Brown FD, Rozelle AL, Yin HL, Balla T and Donaldson JG**. 2001. Phosphatidylinositol 4,5-bisphosphate and Arf6-regulated membrane traffic. The Journal of Cell Biology **154**: 1007-1018. 10.1083/jcb.200103107

55. **Hibino K, Shibata T, Yanagida T and Sako Y**. 2011. Activation Kinetics of RAF Protein in the Ternary Complex of RAF, RAS-GTP, and Kinase on the Plasma Membrane of Living Cells: SINGLE-MOLECULE IMAGING ANALYSIS. Journal of Biological Chemistry **286**: 36460-36468. 10.1074/jbc.M111.262675

56. **Wills MKB and Jones N**. 2012. Teaching an old dogma new tricks: twenty years of Shc adaptor signalling. Biochem. J. **447**: 1-16.

57. **Veithen A, Amyere M, Van Der Smissen P, Cupers P and Courtoy PJ**. 1998. Regulation of macropinocytosis in v-Src-transformed fibroblasts: cyclic AMP selectively promotes regurgitation of macropinosomes. Journal of Cell Science **111**: 2329-2335.

58. **Mettlen M, Platek A, Van Der Smissen P, Carpentier S, Amyere M, Lanzetti L, De Diesbach P, Tyteca D and Courtoy PJ**. 2006. Src Triggers Circular Ruffling and Macropinocytosis at the Apical Surface of Polarized MDCK Cells. Traffic **7**: 589-603. 10.1111/j.1600-0854.2006.00412.x

59. **Wooten MW, Seibenhener ML, Mamidipudi V, Diaz-Meco MT, Barker PA and Moscat J**. 2001. The Atypical Protein Kinase C-interacting Protein p62 Is a Scaffold for NF-κB Activation by Nerve Growth Factor. Journal of Biological Chemistry **276**: 7709-7712. 10.1074/jbc.C000869200

60. **Roskoski J, R.** 2005. Src kinase regulation by phosphorylation and dephosphorylation. Biochemical and Biophysical Research Communications **331**: 1-14.
61. **Chellaiah MA and Schaller MD**. 2009. Activation of Src kinase by protein–tyrosine phosphatase–PEST in osteoclasts: Comparative analysis of the effects of bisphosphonate and protein–tyrosine phosphatase inhibitor on Src activation in vitro. Journal of Cellular Physiology **220**: 382-393. 10.1002/jcp.21777
62. **Mandal A, Shahidullah M, Beimgraben C and Delamere NA**. 2011. The effect of endothelin-1 on Src-family tyrosine kinases and Na,K-ATPase activity in porcine lens epithelium. Journal of Cellular Physiology **226**: 2555-2561. 10.1002/jcp.22602
63. **Wennerberg K and Der CJ**. 2004. Rho-family GTPases: it's not only Rac and Rho (and I like it). J. Cell Sci. **117**: 1301-1312.
64. **Raftopoulou M and Hall A**. 2004. Cell migration: Rho GTPases lead the way. Developmental Biology **265**: 23-32. 10.1016/j.ydbio.2003.06.003
65. **Maekawa M, Ishizaki T, Boku S, Watanabe N, Fujita A, Iwamatsu A, Obinata T, Ohashi K, Mizuno K and Narumiya S**. 1999. Signaling from Rho to the Actin Cytoskeleton Through Protein Kinases ROCK and LIM-kinase. Science **285**: 895-898. 10.1126/science.285.5429.895
66. Feltrin D and Pertz O: Assessment of Rho GTPase Signaling During Neurite Outgrowth. In: Rivero F (ed) Rho GTPases. Springer New York, 2012, pp 181-194.
67. **Sun Y, Lim Y, Li F, Liu S, Lu J-J, Haberberger R, Zhong J-H and Zhou X-F**. 2012. ProBDNF Collapses Neurite Outgrowth of Primary Neurons by Activating RhoA. PLoS ONE **7**: e35883. 10.1371/journal.pone.0035883
68. **Wills Zachary P, Mandel-Brehm C, Mardinly Alan R, McCord Alejandra E, Giger Roman J and Greenberg Michael E**. 2012. The Nogo Receptor Family Restricts Synapse Number in the Developing Hippocampus. Neuron **73**: 466-481. http://dx.doi.org/10.1016/j.neuron.2011.11.029
69. **Zhao CF, Liu Y, Ni YL, Yang JW, Hui HD, Sun ZB and Liu SJ**. 2013. SCIRR39 Promotes Neurite Extension via RhoA in NGF-Induced PC12 Cells. Developmental Neuroscience **35**: 373-383.
70. **Manning BD and Cantley LC**. 2007. AKT/PKB Signaling: Navigating Downstream. Cell **129**: 1261-1274. 10.1016/j.cell.2007.06.009
71. **Serrano M, Lin AW, McCurrach ME, Beach D and Lowe SW**. 1997. Oncogenic ras Provokes Premature Cell Senescence Associated with Accumulation of p53 and p16INK4a. Cell **88**: 593-602. 10.1016/s0092-8674(00)81902-9
72. **Overmeyer JH and Maltese WA**. 2011. Death Pathways Triggered by Activated Ras in Cancer Cells. Front. Biosci. **16**: 1693-1713.
73. **D'Souza-Schorey C and Chavrier P**. 2006. ARF proteins: roles in membrane traffic and beyond. Nat Rev Mol Cell Biol **7**: 347-358.
74. **Naslavsky N, Weigert R and Donaldson JG**. 2004. Characterization of a Nonclathrin Endocytic Pathway: Membrane Cargo and Lipid Requirements. Molecular Biology of the Cell **15**: 3542-3552. 10.1091/mbc.E04-02-0151
75. **Funakoshi Y, Hasegawa H and Kanaho Y**. 2011. Regulation of PIP5K activity by Arf6 and its physiological significance. Journal of Cellular Physiology **226**: 888-895. 10.1002/jcp.22482
76. **Ferrari C, Zippel R, Martegani E, Gnesutta N, Carrera V and Sturani E**. 1994. Expression of Two Different Products of CDC25Mm, a Mammalian Ras Activator, during

Development of Mouse Brain. Experimental Cell Research **210**: 353-357. http://dx.doi.org/10.1006/excr.1994.1048

77. **Engelman JA, Luo J and Cantley LC**. 2006. The evolution of phosphatidylinositol 3-kinases as regulators of growth and metabolism. Nat Rev Genet **7**: 606-619.

78. **Jovanovic OA, Brown FD and Donaldson JG**. 2006. An Effector Domain Mutant of Arf6 Implicates Phospholipase D in Endosomal Membrane Recycling. Mol. Biol. Cell **17**: 327-335.

79. **Donepudi M and Resh MD**. 2008. c-Src trafficking and co-localization with the EGF receptor promotes EGF ligand-independent EGF receptor activation and signaling. Cellular Signalling **20**: 1359-1367. 10.1016/j.cellsig.2008.03.007

80. **Saito Y, Tsuzuki K, Yamada N, Okado H, Miwa A, Goto F and Ozawa S**. 2003. Transfer of NMDAR2 cDNAs increases endogenous NMDAR1 protein and induces expression of functional NMDA receptors in PC12 cells. Molecular Brain Research **110**: 159-168. http://dx.doi.org/10.1016/S0169-328X(02)00548-X

81. **Obara Y, Labudda K, Dillon TJ and Stork PJS**. 2004. PKA phosphorylation of Src mediates Rap1 activation in NGF and cAMP signaling in PC12 cells. Journal of Cell Science **117**: 6085-6094. 10.1242/jcs.01527

82. **Arthur DB, Akassoglou K and Insel PA**. 2006. P2Y2 and TrkA receptors interact with Src family kinase for neuronal differentiation. Biochemical and Biophysical Research Communications **347**: 678-682.

83. **Tsuruda A, Suzuki S, Maekawa T and Oka S**. 2004. Constitutively active Src facilitates NGF-induced phosphorylation of TrkA and causes enhancement of the MAPK signaling in SK-N-MC cells. FEBS Letters **560**: 215-220. 10.1016/s0014-5793(04)00115-2

84. **Spiering D and Hodgson L**. 2011. Dynamics of the Rho-family small GTPases in actin regulation and motility. Cell Adhesion & Migration **5**: 170-180.

85. **Knippschild U, Gocht A, Wolff S, Huber N, Löhler J and Stöter M**. 2005. The casein kinase 1 family: participation in multiple cellular processes in eukaryotes. Cellular Signalling **17**: 675-689.

86. **Kurokawa K and Matsuda M**. 2005. Localized RhoA Activation as a Requirement for the Induction of Membrane Ruffling. Molecular Biology of the Cell **16**: 4294-4303. 10.1091/mbc.E04-12-1076

87. **Vander Heiden MG, Cantley LC and Thompson CB**. 2009. Understanding the Warburg Effect: The Metabolic Requirements of Cell Proliferation. Science **324**: 1029-1033. 10.1126/science.1160809

88. **Yung Yun C, Stoddard Nicole C, Mirendil H and Chun J**. 2015. Lysophosphatidic Acid Signaling in the Nervous System. Neuron **85**: 669-682. http://dx.doi.org/10.1016/j.neuron.2015.01.009

880 **Figure Legends**

881 **Figure 1. NGF-induced macropinosomes co-internalize dextran with 0.5 µm latex beads**
882 **and contain both PIP2 and PIP3.** Cells were co-treated with Alexa^{546}-transferrin and Alexa^{488}-
883 Dextran **(A)**, Alexa^{488}-dextran and 0.5 µm Alexa^{546}-latex beads (10 ng) **(B)**, or transfected with
884 **(C)** EGFP alone, **(D)** EGFP-tagged constructs encoding the PH domain of AKT (PIP_3 tracer), the
885 PH domain of PLD (PIP_2 tracer) or **(E)** EGFP-Clathrin. Alexa^{546}-dextran was given as a fluid
886 tracer and cells were stimulated with 100ng/ml NGF (24h) and visualized by confocal
887 microscopy. Scale bar = 10 µm.

888 **Figure 2. NGF-stimulated Daoy-TrkA cells activate both Rac and H-Ras.** Daoy-TrkA cells
889 were stimulated with 100 ng/ml NGF and lysates harvested at 10 min, 6 h, 12 h and 24 h. **(A, B)**
890 Lysates were assayed for activation of H-Ras and Rac using GST fusion proteins that will only
891 bind active Rac1 (Pak-1-CRIB) **(A)** and Ras (RBD) **(B)**. Pulldowns (500 µg) and whole cell
892 lysates (WCL) (25 µg) were analyzed on 12% SDS gels and westerns probed with the indicated
893 antibodies. WCLs were assayed for changes in the expression of each GTPase, relative to β-
894 actin, at each time point. Changes in the activation of each GTPase were determined relative to
895 levels of expression normalized to β-actin. **(C)** Direct comparison between the activation of Rac
896 (less than 1-fold) relative to H-Ras (3 to 7-fold) during the same time period. Asterisks (*)
897 indicates a statistically significant P-value < 0.05 increase relative to un-stimulated cells as
898 performed using one-way ANOVA and Post-Tukey test.

899 **Figure 3. Expression of DN-H-Ras, and Rab5 blocks and Arf6 reduces the size of NGF-**
900 **induced Macropinosomes. (A)** EGFP-tagged DN GTPases (H-Ras, Arf6, Rab5, Rap1b, Rab7,
901 Rac1, Arf1, Rab34, Dyn2, Cdc42, CtBP1/BARS) were transfected into Daoy-TrkA cells and
902 assayed for changes in both NGF-induced macropinosomes and the uptake of Alexa^{546}-dextran

903 relative to cells transfected with EGFP at 24 h. Scale bar = 10 µm. **(B)** The Rac specific
904 inhibitor, EHT1864 (10 µM), was assayed for changes in both NGF-induced vacuole formation
905 at 24 h (phase contrast microscopy) as well as changes in the activation of Rac at 6 h in a
906 pulldown assay. Asterisk (*) indicates a statistically significant *P*-value < 0.05 increase in Rac
907 activation at 6h, relative to un-stimulated cells, as well as a significant decrease in activity in the
908 presence of EHT1864, as performed using one-way ANOVA and Post-Tukey test.

909 **Figure 4. CA-Ras Mimics NGF-induced Macropinocytosis in Daoy-TrkA Cells. (A)** EGFP-
910 tagged CA-Ras and CA-Arf6, but not CA-Rac1, Rab34, Cdc42 or Rap1b, induces NGF-
911 independent macropinocytosis and Alexa^{546}-dextran uptake comparable to cells transfected with
912 EGFP and NGF stimulated (24 h). **(B)** CA-Ras-EGFP, but not CA-Arf6-EGFP, induced
913 macropinosomes are blocked by the CK1 inhibitor D4476. **(C)** CA-Arf6-EGFP induced
914 macropinosomes contain both PIP_3 (PH-AKT-mCherry) and PIP_2 (PH-PLD-mCherry). **(D)** The
915 majority of CA-Ras-EGFP induced macropinosomes do not contain PIP_3 (PH-AKT-mCherry)
916 and/or PIP_2 (PH-PLD-mCherry) (white arrows). **(E)** EGFP tagged RBD of c-Raf-1 localizes
917 active Ras in the initial lamellipodia, the macropinosmes as well as large, fused vacuoles in the
918 presence of NGF. **(F)** The EGFP-tagged cRaf-1 CRD ($R^{89}A$) mutant, which cannot bind active
919 Ras, is diffusely found throughout the cytosol in the presence of NGF. Scale bar = 10 µm.

920 **Figure 5. siRNA mediated Knockdown of H-Ras but Neither Cdc42 nor Rac1 Blocks NGF-**
921 **induced Macropinosomes. (A)** Daoy-TrkA cells were transfected with siRNAs against Cdc42,
922 Rac1 and a stealth control and changes in protein expression assayed by Western blot at 48 h. **(B)**
923 Daoy-TrkA cells were co-transfected with a Cy3 (red) control siRNA and either a non-specific
924 siRNA (LC3) or siRNAs against both Cdc42 and Rac1. Cells were either left un-stimulated or
925 treated with NGF and changes in Alexa^{488}-Dextran uptake examined in Cy3 positive cells at 24

h. **(C)** Lysates from Daoy-TrkA cells were examined to determine if they express 1 or all 3 Ras isoforms relative to Hela cell lysates as a control. **(D)** siRNA to H-Ras effectively reduce H-Ras expression. **(E)** Daoy-TrkA cells were co-transfected with a Cy3 (red) control siRNA and either a non-specific siRNA (LC3) or the H-Ras siRNA. Cells were either left un-stimulated or treated with NGF and changes in Alexa^{488}-Dextran uptake examined in Cy3 positive cells at 24 h. Scale bar = 10 μm.

Figure 6. FRS2, not ShcA, Binding to the Phosphorylated Juxtamembrane Tyrosine Residue, Tyr^{490}, is Essential to H-Ras Activation by TrkA. (A) Schematic showing that FRS2 and Shc bind competitively to pTyr^{490} following TrkA activation. **(B)** Daoy-TrkA cells express ShcA, but not ShcB or ShcC. siRNAs for both human ShcA and FRS2 effectively reduce expression of their respective targets in transfected Daoy-TrkA cells relative to the siRNA control. **(C)** Daoy-TrkA cells were co-transfected with a Cy3 control siRNA and either a non-specific siRNA (LC3) or the siRNAs against ShcA or FRS2. Cells were either left un-stimulated or treated with NGF and changes in Alexa^{488}-Dextran uptake examined in Cy3 positive cells at 24 h. Scale bar = 10 μm.

Figure 7. Src Activation, *via* FRS2, is Essential to NGF-dependent Macropinocytosis and Cell Death. (A) Schematic showing that Src is recruited into TrkA signaling *via* FRS2 and this facilitates activation of H-Ras. **(B)** Daoy-TrkA cells were treated with PP2 or DMSO (1 h) prior to addition of NGF and incubated for an additional 12 h. Cells were scored for cell death using the trypan blue exclusion assay (N=3). **(C)** Daoy-TrkA cells were treated as described in **B**, lysed and analyzed by Western blot for TrkA phosphorylation, at p Y^{490}, relative to β-actin. **(D)** Daoy-TrkA cells were either left untreated or pre-treated with D4476 (1 h) prior to NGF stimulation. Lysates were analyzed for changes in the phosphorylation status of Src (Y^{416})

relative to total levels of Src and β-actin. **(E)** Daoy-TrkA cells were transfected with a Src siRNA or a Src scramble control for 24 h (left panel) or up to 72 h (right panel) and changes in Src expression determined by Western blot relative to β-actin. **(F)** Daoy-TrkA cells were co-transfected with a Cy3 control siRNA and either a scramble siRNA or the Src siRNA. Cells were either left un-stimulated or treated with NGF and changes in Alexa^{488}-Dextran uptake were examined in Cy3 positive cells at 24 h. **(G)** Daoy-TrkA cells were transfected with EGFP-tagged WT or DN-Src and left untreated or stimulated with NGF and Alexa^{546}-Dextran for 24 h prior to examining changes in macropinocytosis. Scale bar = 10 μm.

Figure 8. RhoB maintains Actin-Stress Fibers and must be Inactivated *via* CK1-dependent Phosphorylation at Ser^{185} to enable NGF-induced Macropinocytosis. (A) Daoy-TrkA cells were stimulated with NGF, lysates harvested at 10 min, 6 h, 12 h and 24 h and assayed for activation of RhoB using GST-Rhoteckin *vs* GST alone. Pulldowns and WCLs were analyzed on 12% SDS gels and blots probed with the indicated antibodies. WCLs were also assayed for changes in expression of RhoB, relative to β-actin, at each time point. **(B)** Daoy-TrkA cells were transfected with EGFP, EGFP-tagged CA-RhoB (Q^{63}L) and the EGFP-tagged site directed RhoB mutant (S^{185}A). Cells were stimulated with NGF and Alexa^{546}-Dextran added for 24 h prior to examining changes in macropinocytosis. **(C)** Daoy-TrkA cells were transfected with control or RhoB siRNA and changes in RhoB expression examined by Western blot at 24h. **(D)** Cells were co-transfected with Cy3 control siRNA and either a control siRNA or the RhoB siRNA. Cells were treated with NGF and Alexa^{488}-Dextran uptake examined in Cy3 positive cells at 24 h. Scale bar = 10 μm.

Figure 9. RhoA Activation Drives Lamellopodia Formation and is Essential to NGF-Induced Macropinocytosis in Daoy-TrkA Cells. (A) Daoy-TrkA cells were stimulated with

NGF, lysates harvested at 10 min, 6 h, 12 h and 24 h and assayed for activation of RhoA using GST-Rhoteckin *vs* GST alone. Pulldowns and WCLs were analysed on 12% SDS gels and blots probed with the indicated antibodies. WCLs were also assayed for changes in expression of RhoA, relative to β-actin, at each timepoint. **(B)** Daoy-TrkA cells were transfected with an EGFP-tagged reporter construct encoding the RhoA binding domain of Rhoteckin to visualize active RhoA (GFP-rGBD). Cells were examined by confocal microscopy in the absence or presence of NGF stimulation at 24 h. **(C)** Daoy-TrkA cells were transfected with YFP-tagged DN RhoA ($T^{19}N$), treated with $Alexa^{546}$-dextran, stimulated with NGF and visualized by confocal microscopy at 24 h. **(D)** Daoy-TrkA cells were treated with the Rho inhibitor CT04 (2 µg/ml) for 1 h prior to stimulating cells with NGF for 4 h. Cells were visualized for macropinosomes by phase contrast microscopy. Scale bar = 10 µm.

Figure 10. Schematic of TrkA-dependent signaling pathways that drive macropinocytosis.

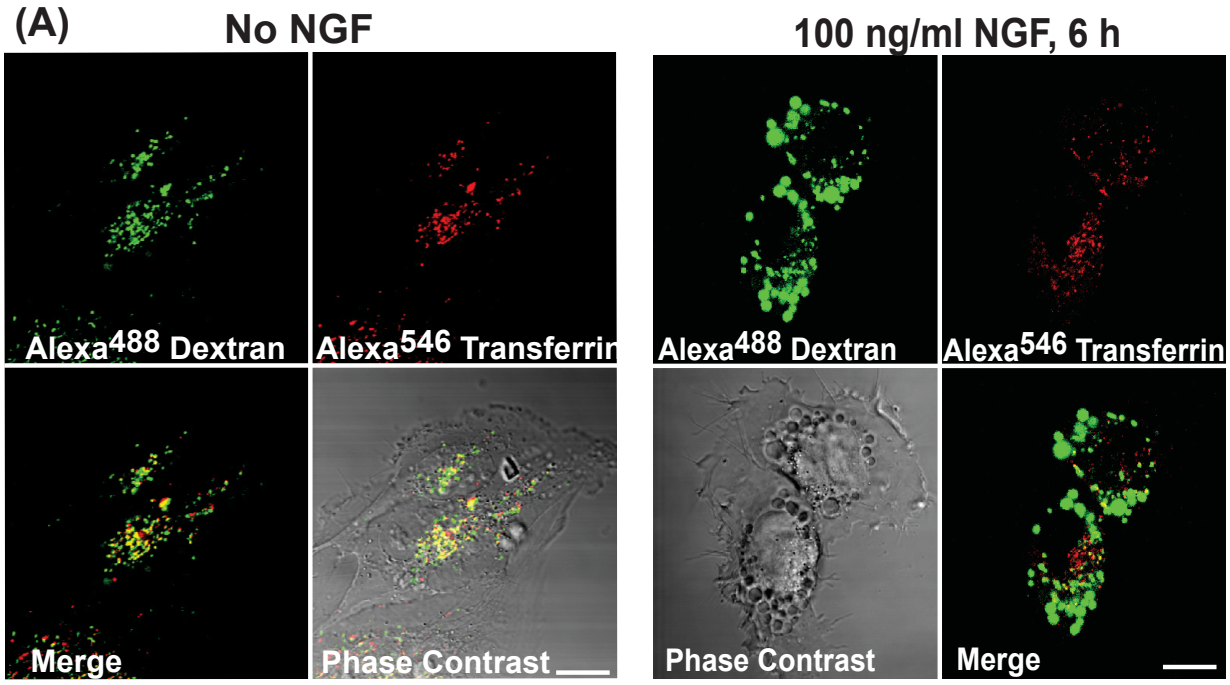

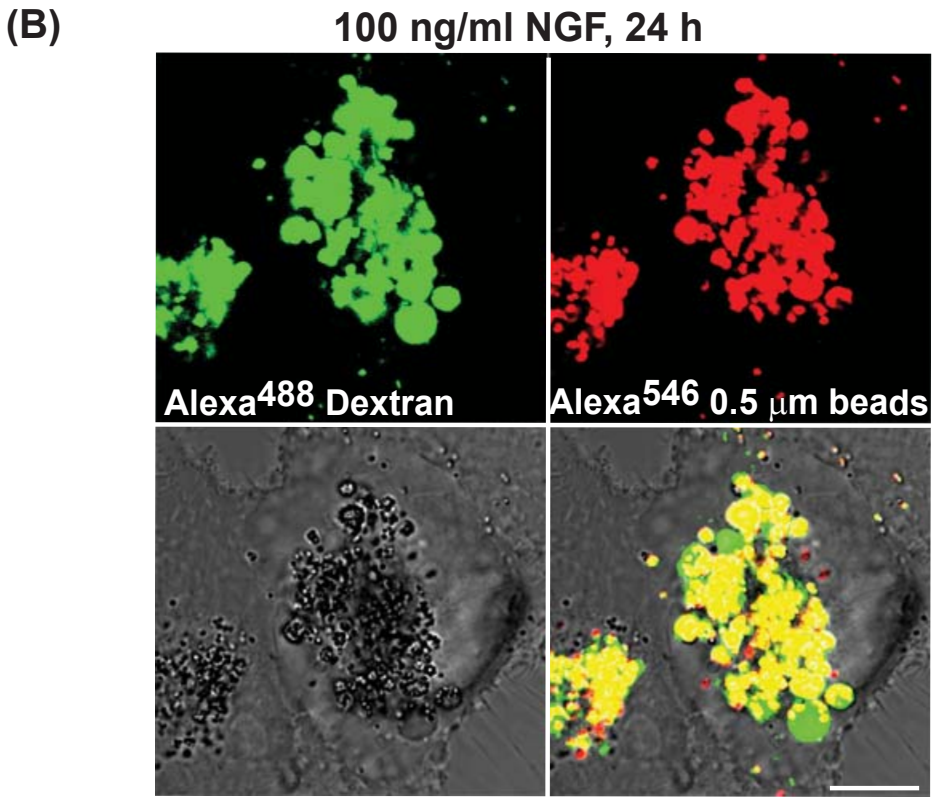

Figure 1.

Molecular and Cellular Biology

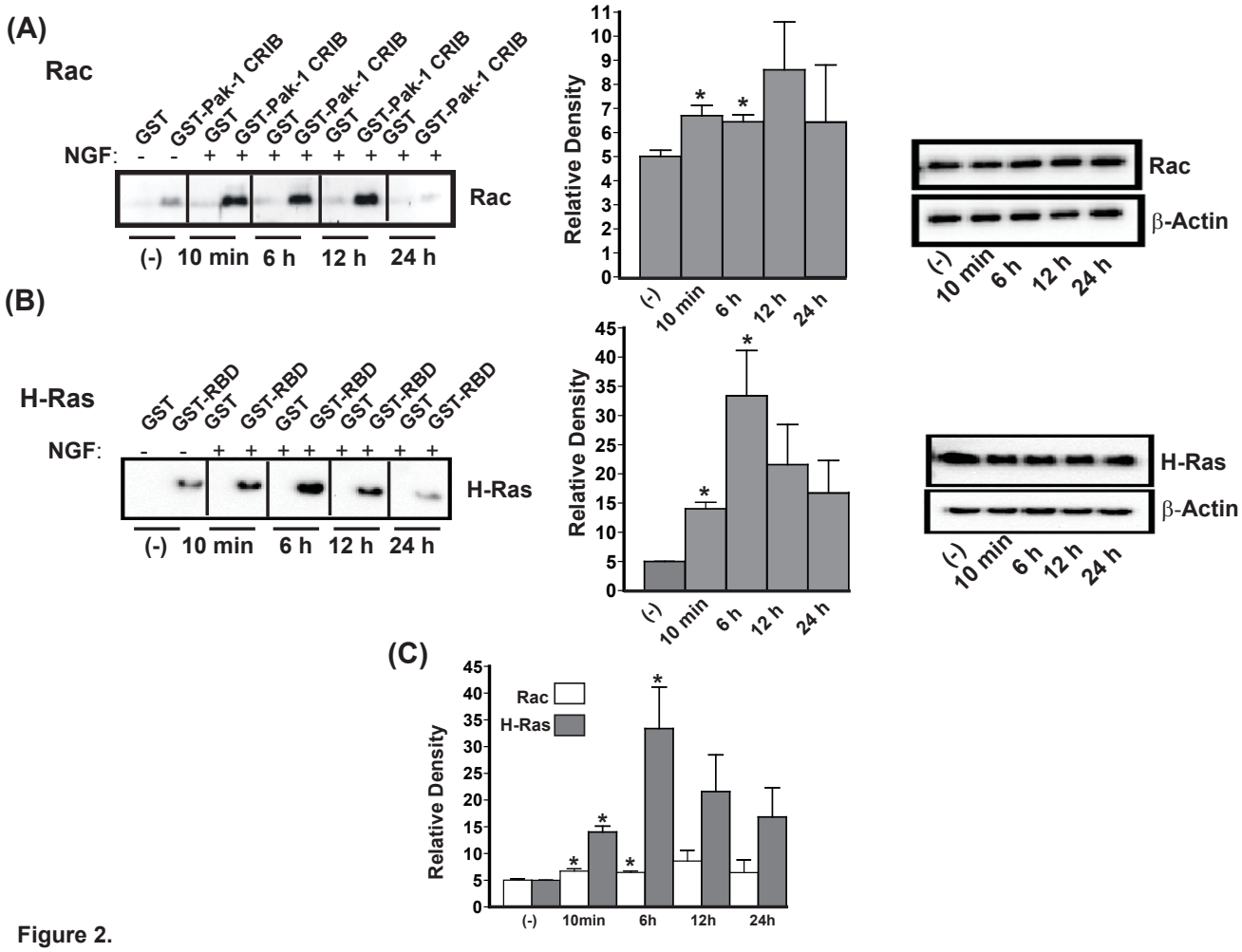

Figure 2.

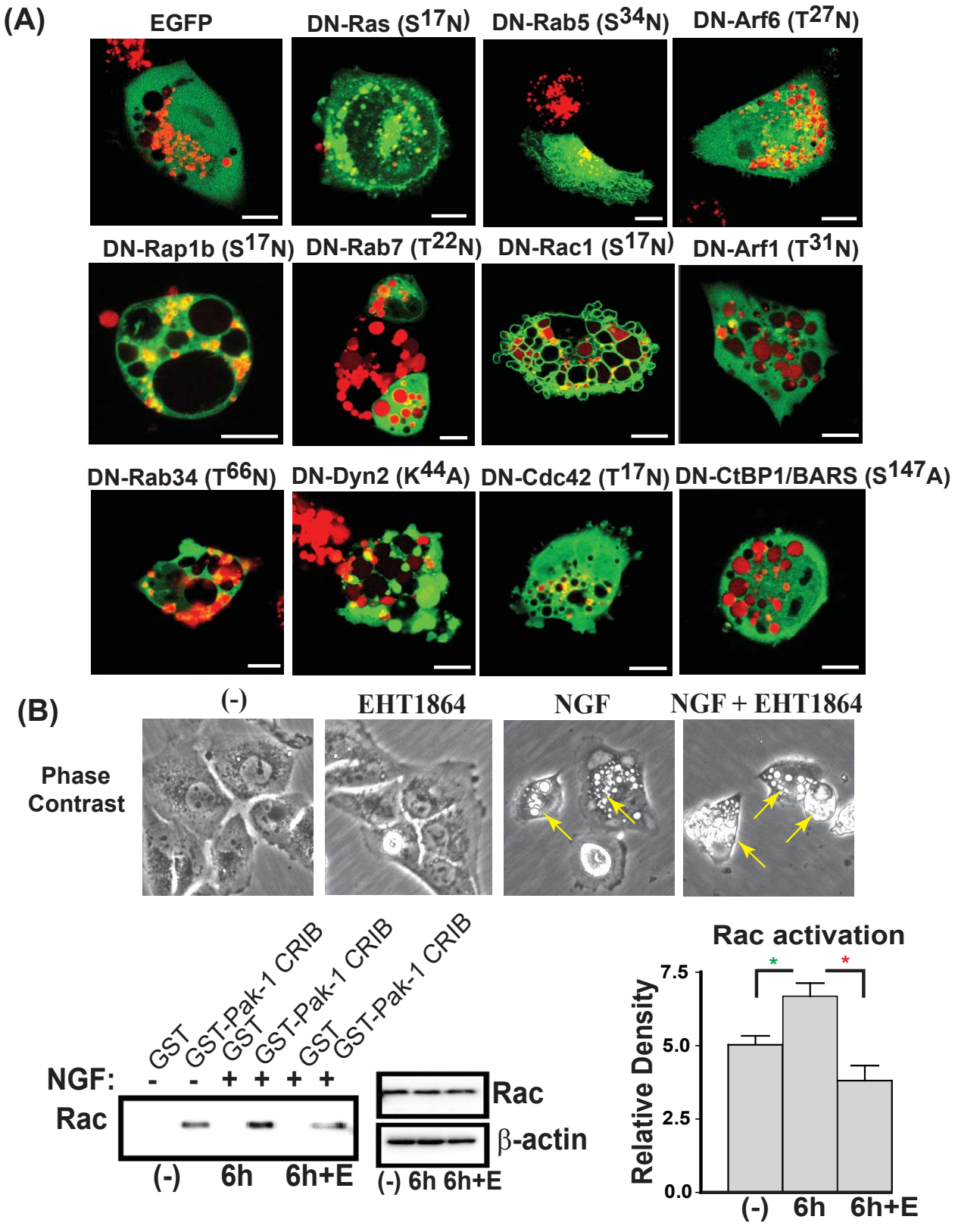

Figure 3.

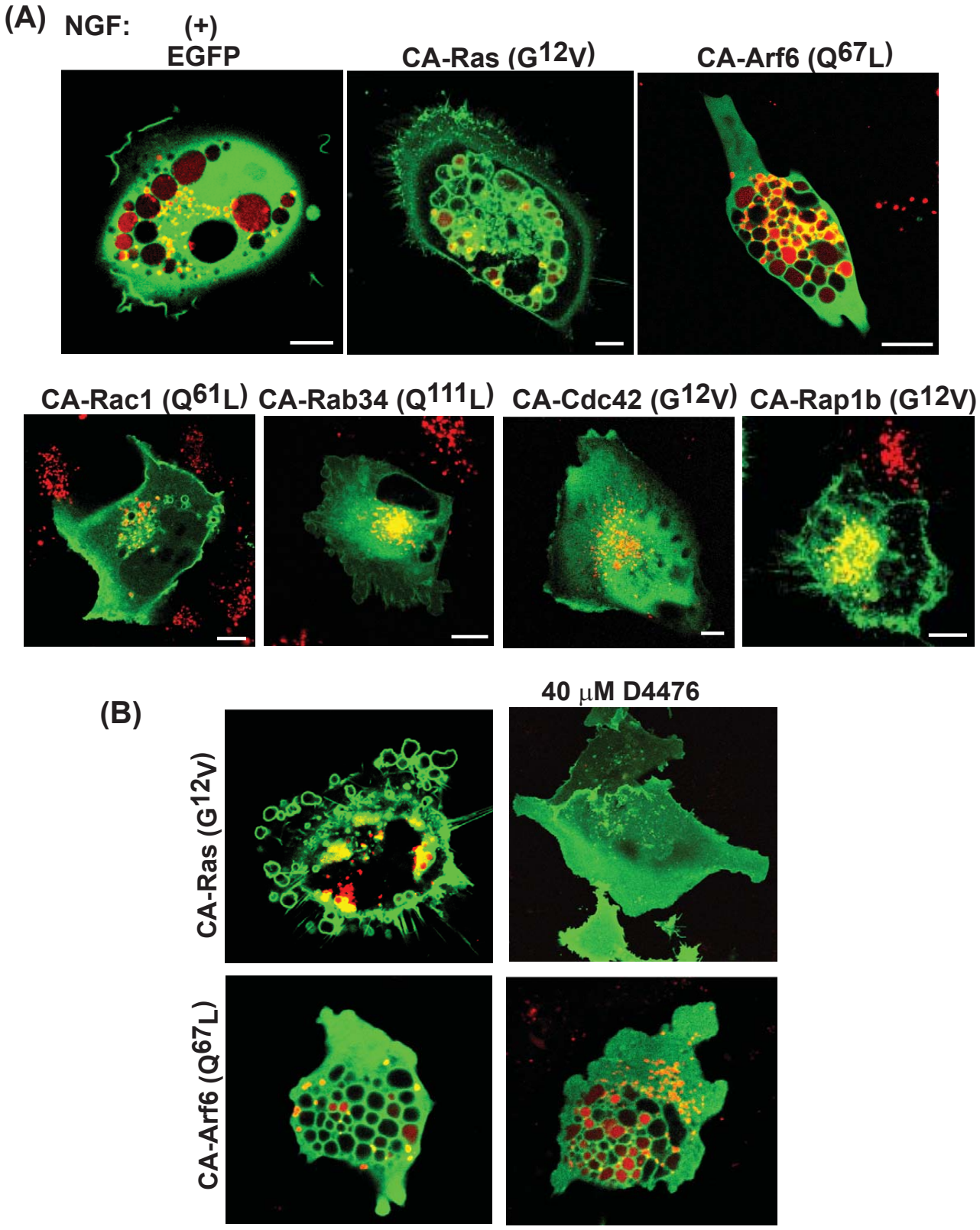

Figure 4.

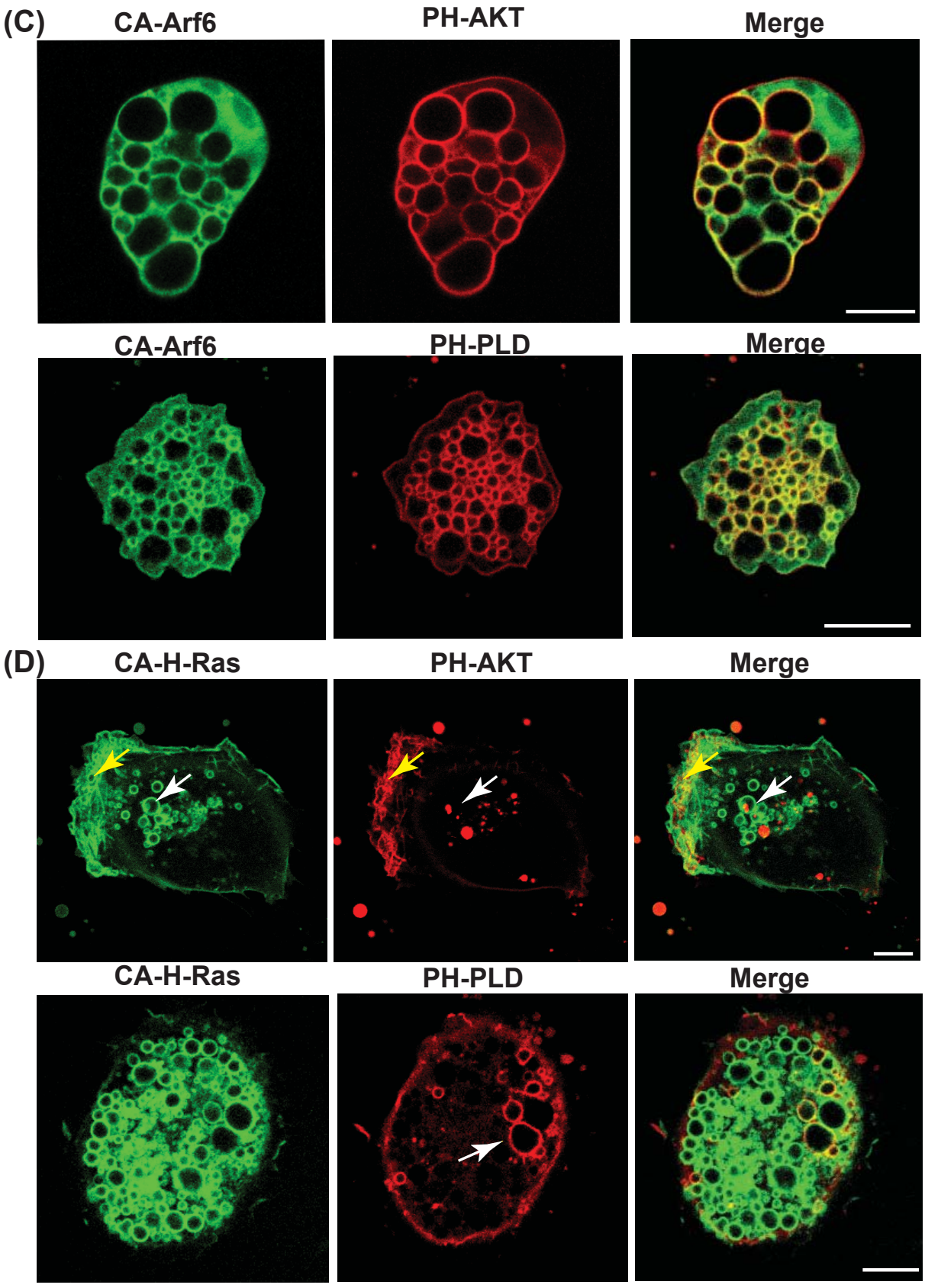

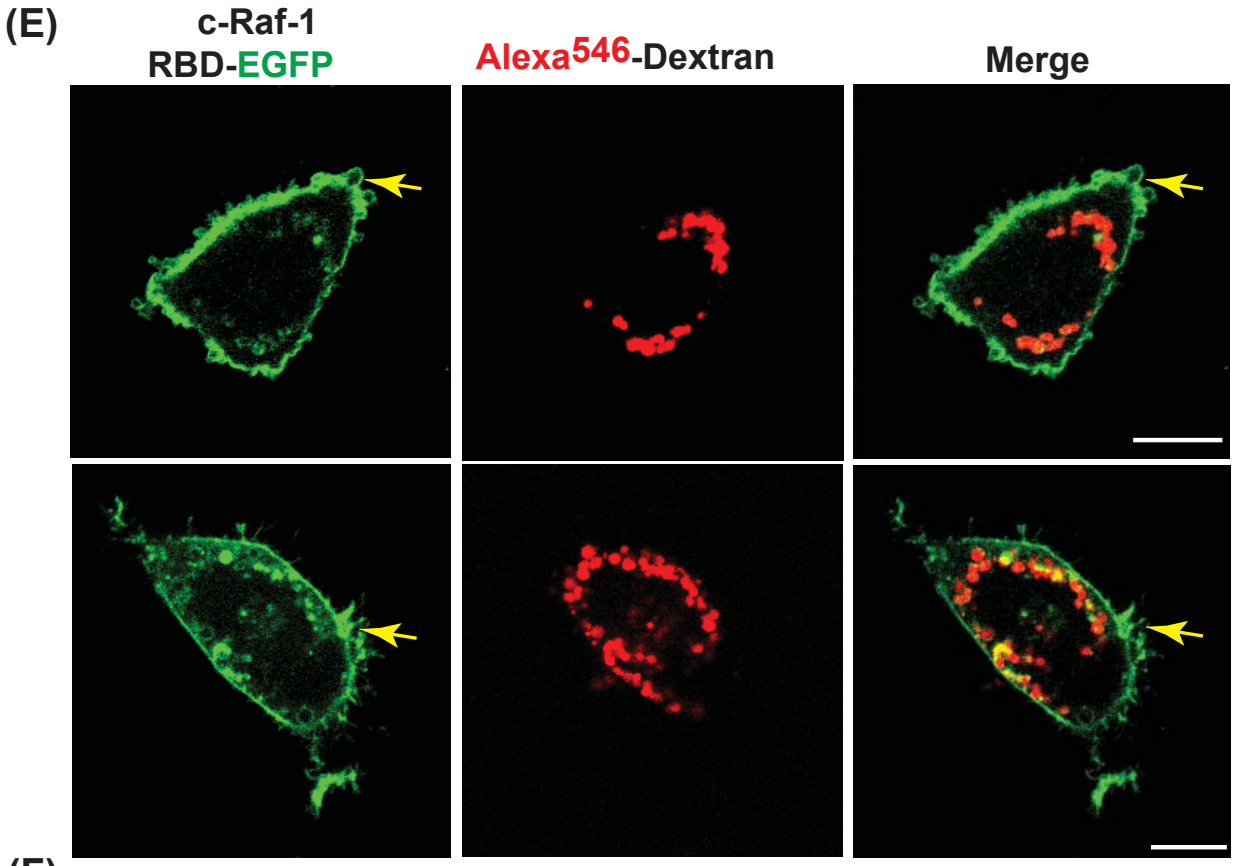

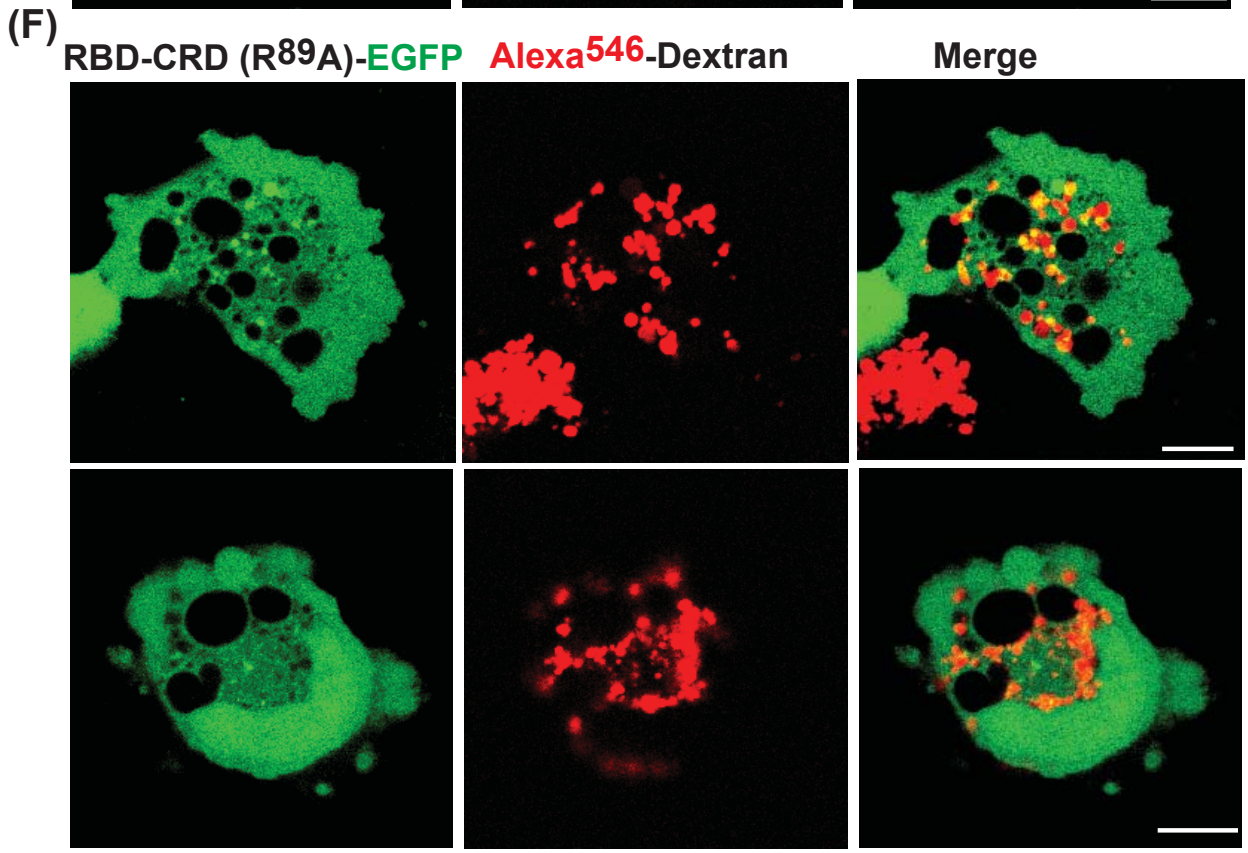

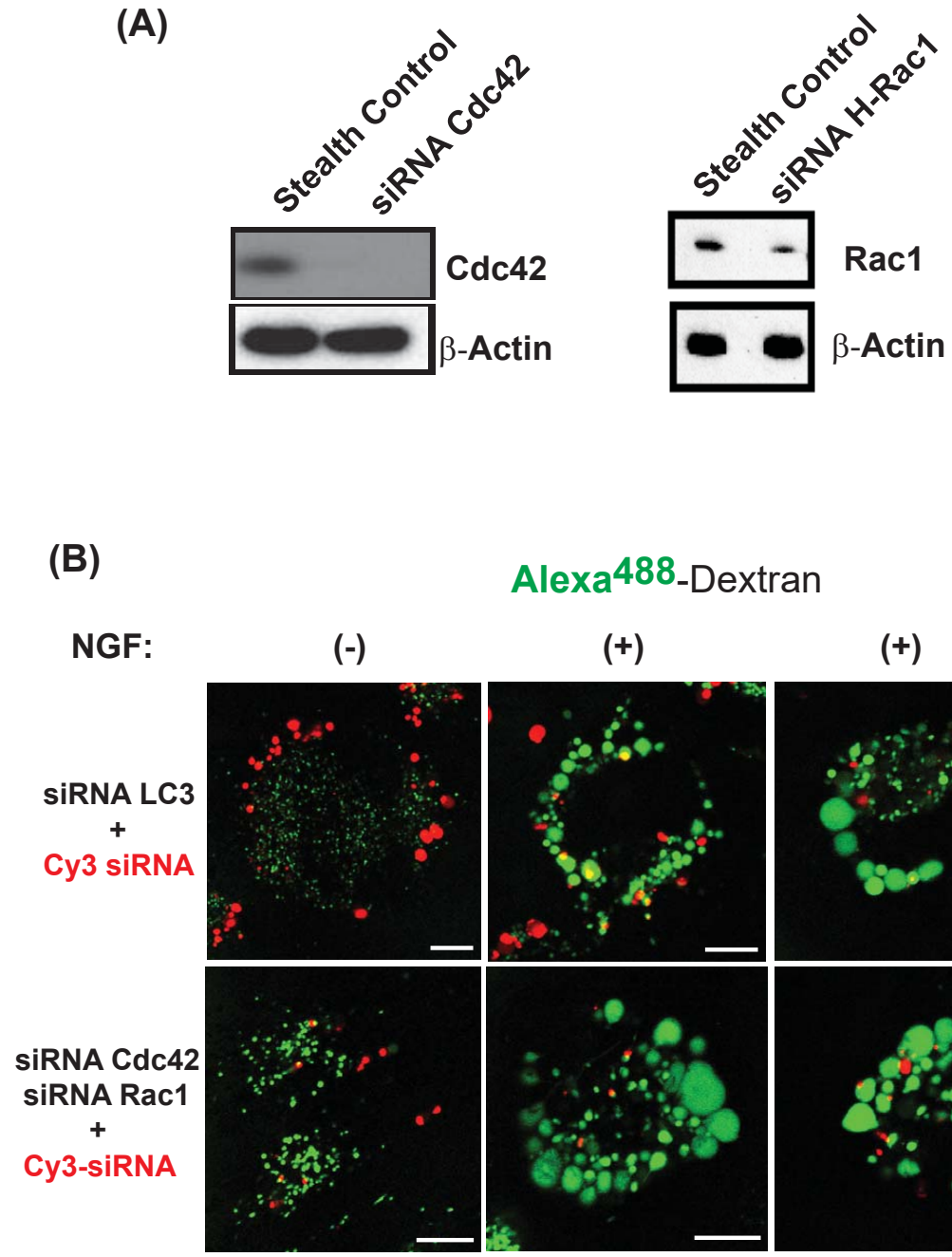

Figure 5

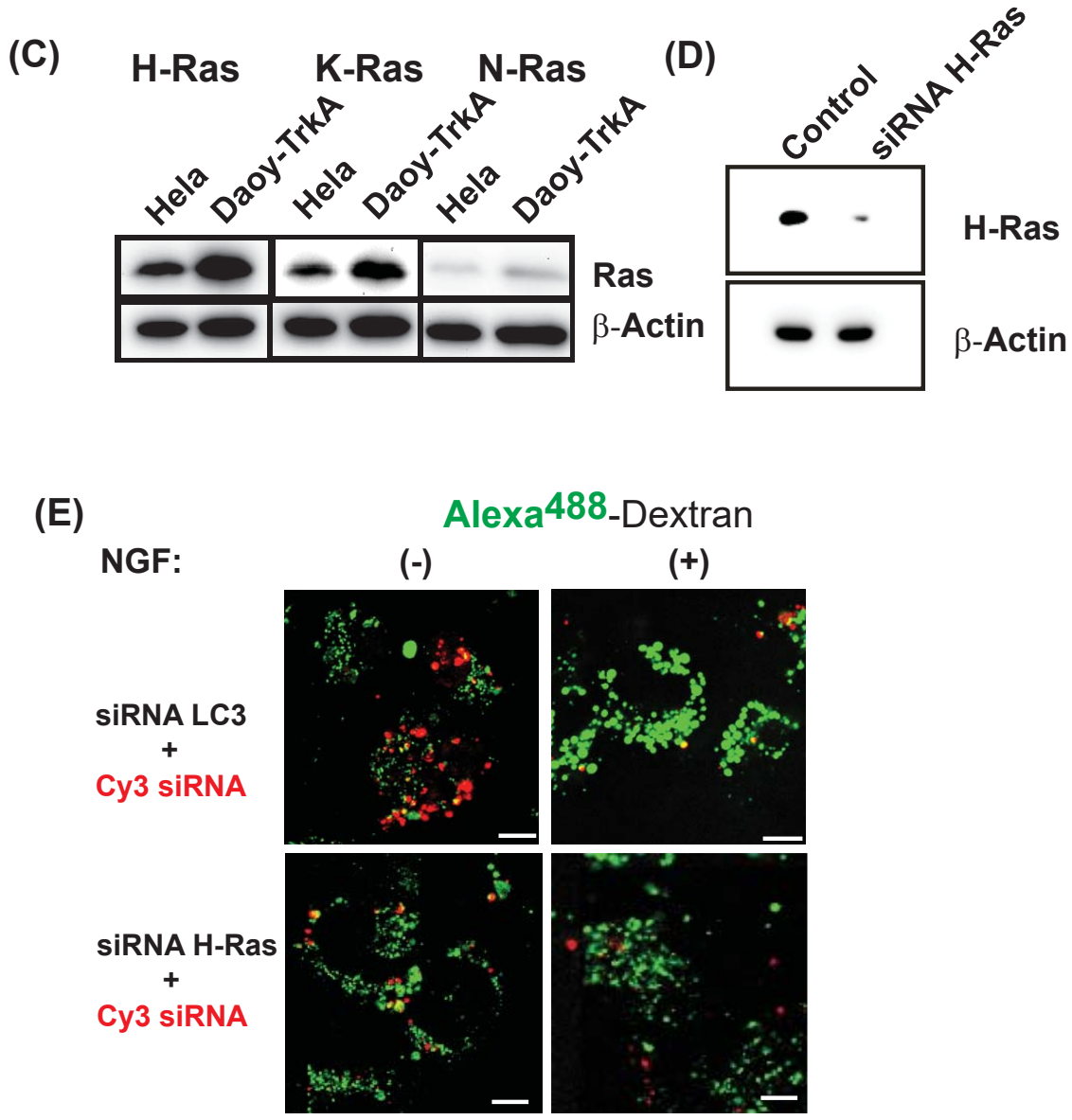

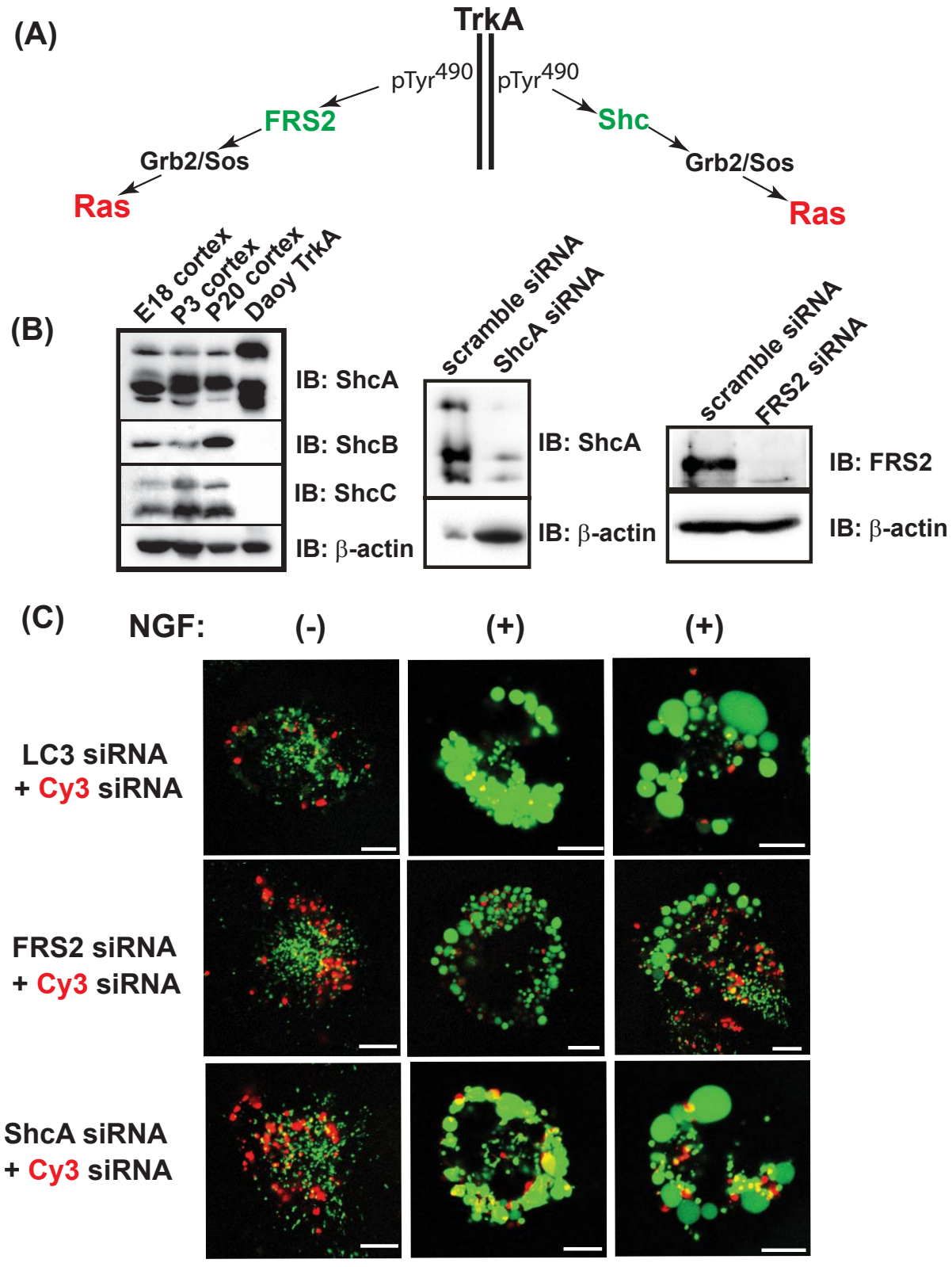

Figure 6.

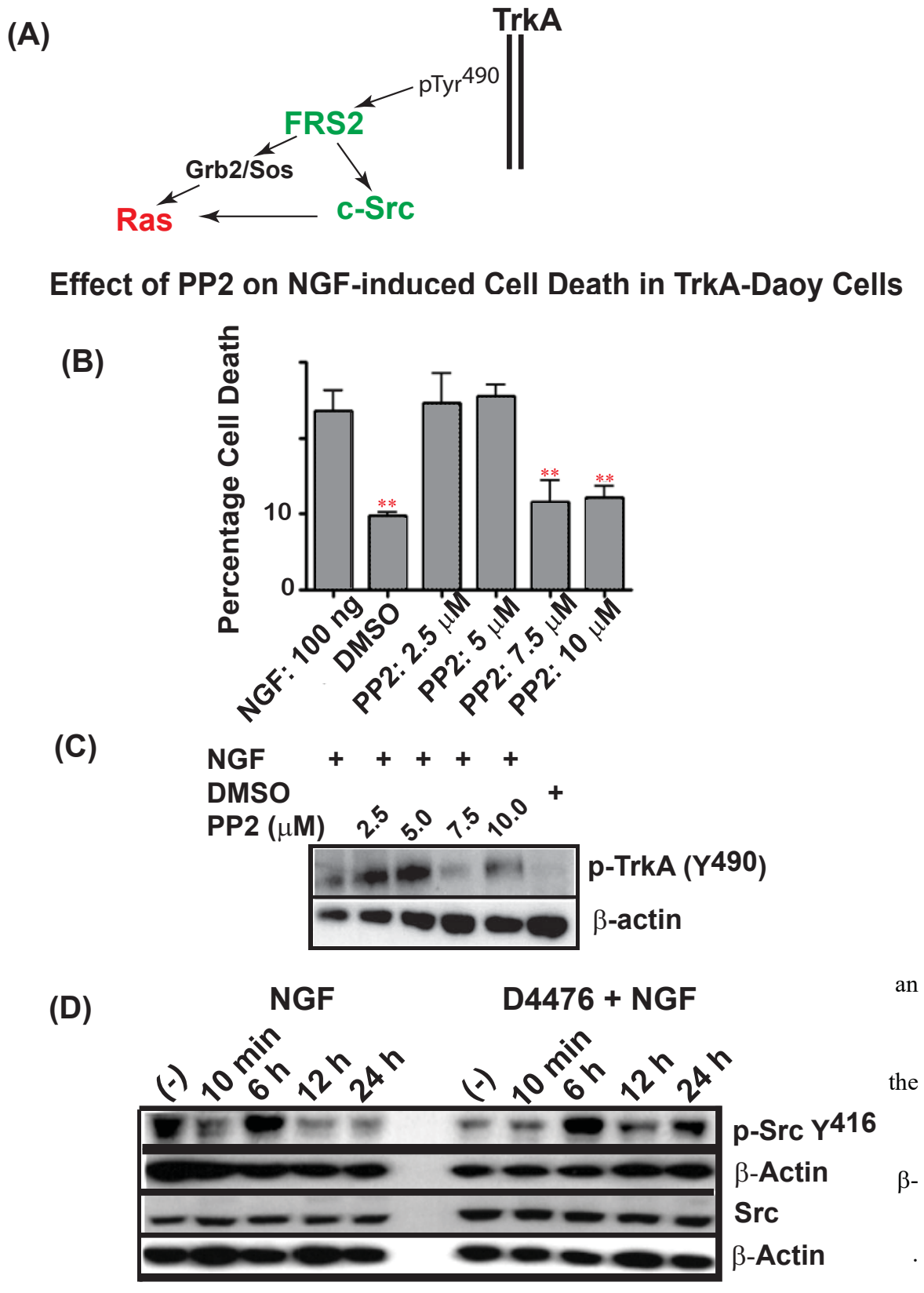

an

the

β-

.

Figure 7.

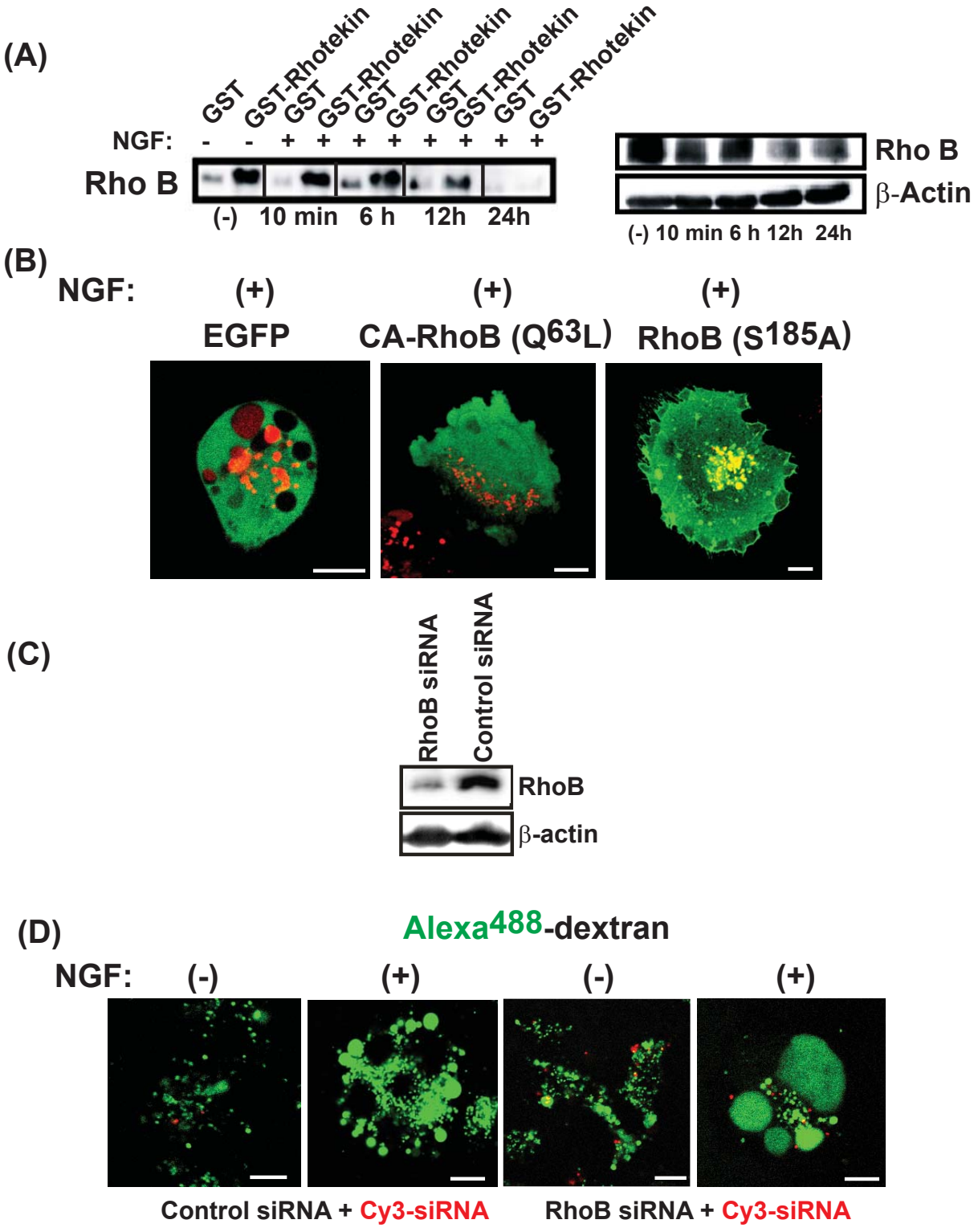

Figure 8.

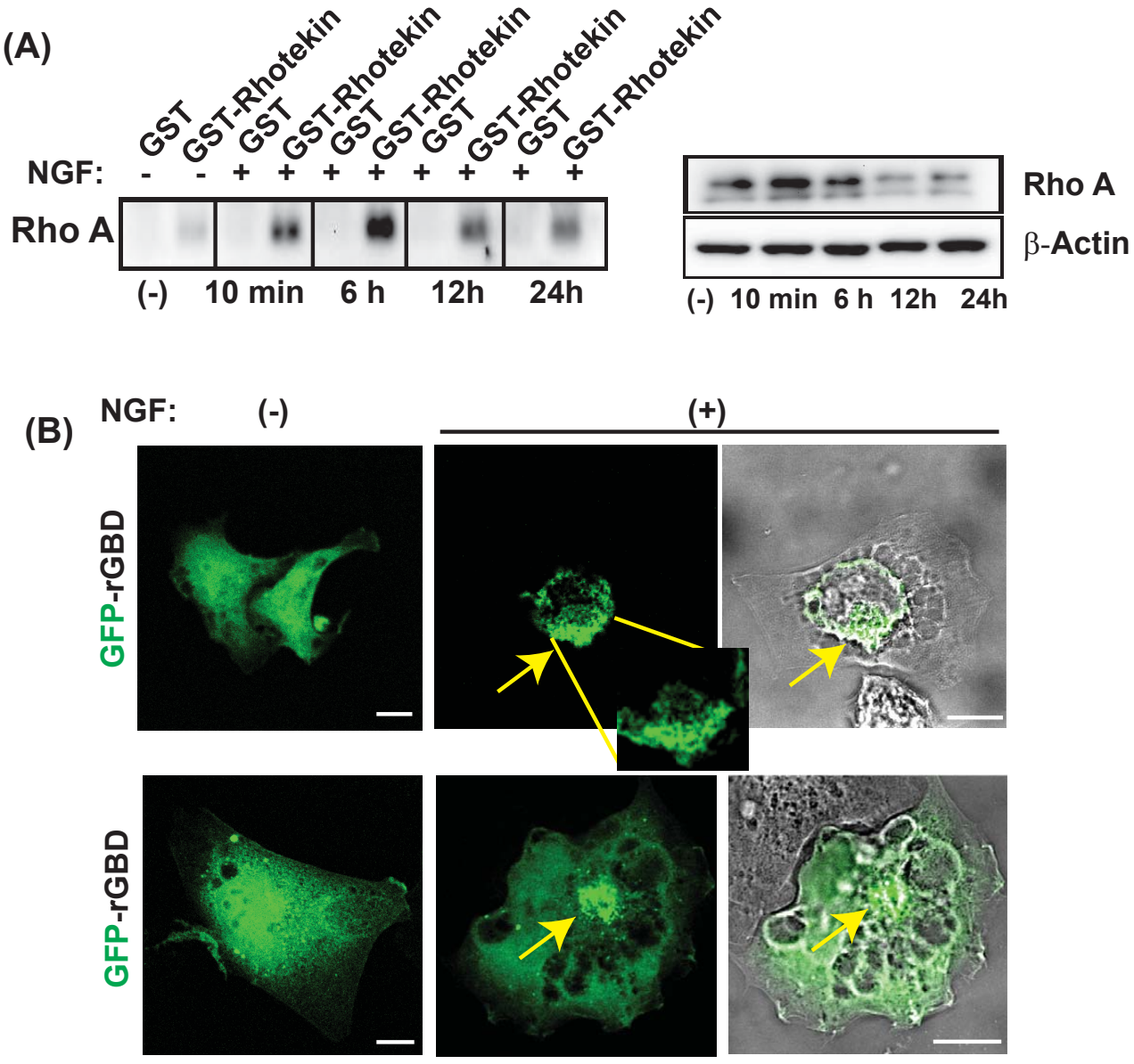

Figure 9.

Molecular and Cellular Biology

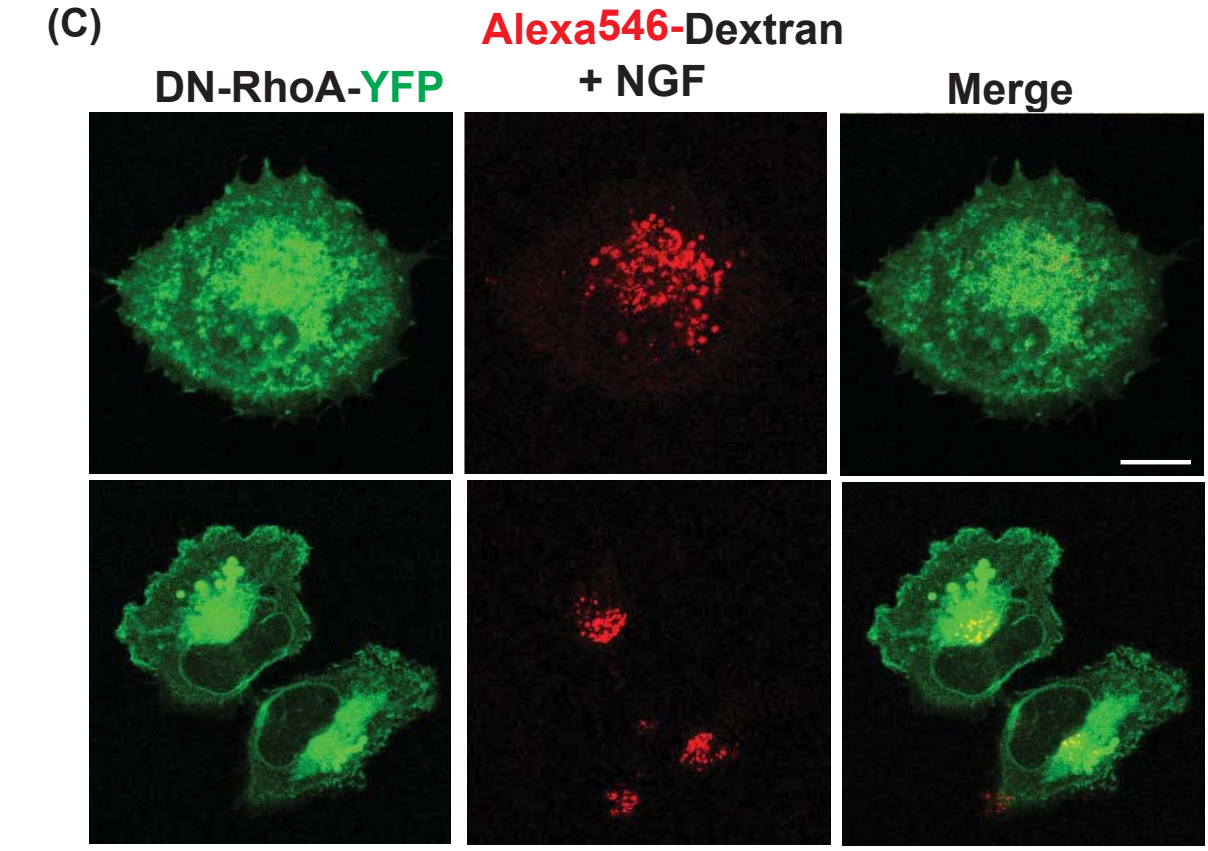

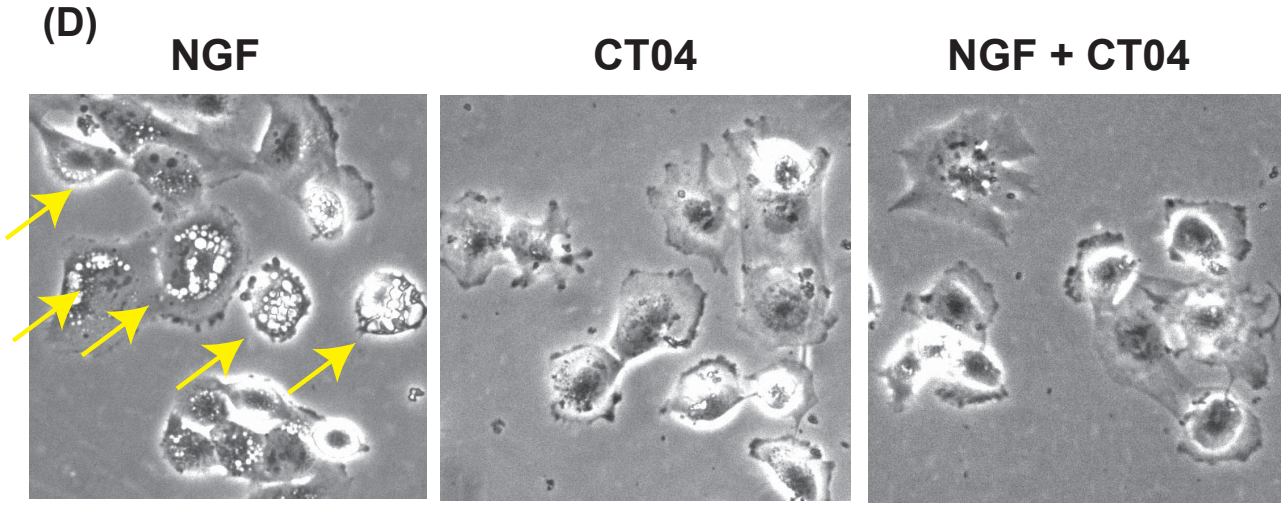

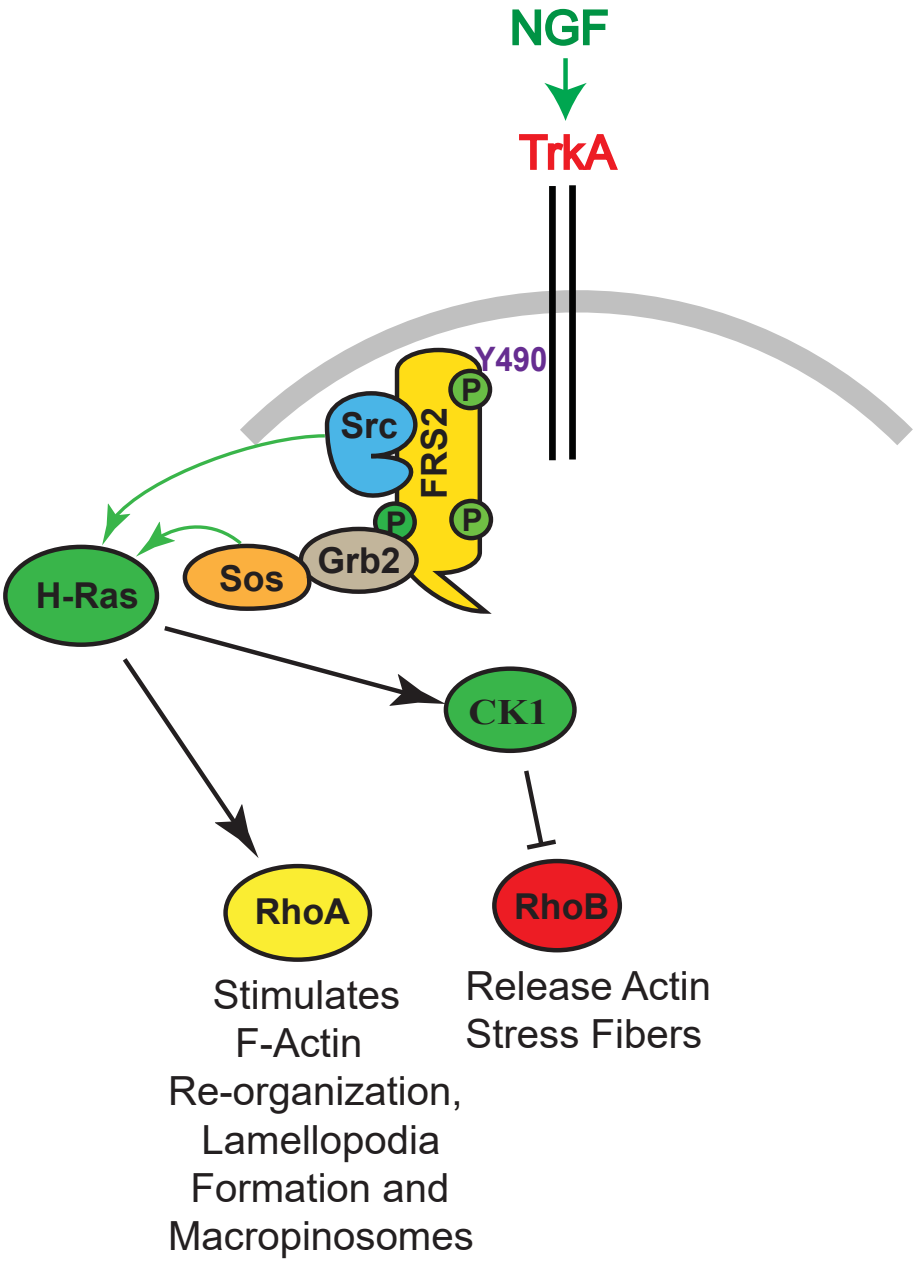

Figure 10.